2021

# Producing a theoretical model for determining the appropriate propeller for a given model aircraft application

Bright, Florian

Bright, F. (2021) 'Producing a theoretical model for determining the appropriate propeller for a given model aircraft application', The Plymouth Student Scientist, 14(1), pp.165-205.
http://hdl.handle.net/10026.1/17333

The Plymouth Student Scientist
University of Plymouth

# Producing a theoretical model for determining the appropriate propeller for a given model aircraft application

Florian Bright

*Project Advisor: Adam Kyte, School of Engineering, Computing and Mathematics, Faculty of Science and Engineering, University of Plymouth, Drake Circus, Plymouth, PL4 8AA*

## Abstract

This paper investigates a method of determining the most suitable propeller for any given model aircraft application based on simple inputs such as desired airspeed and powerplant requirements. This method has been embodied through a spreadsheet-based tool which is directed at the end users of model aircraft for establishing the propeller that will best suit their specific needs. The aims of this paper have been addressed through the aid of a case study, which outlines specific operating conditions and assists in putting the background theory into perspective. The ultimate goal for the case study was to determine the most suitable off-the-shelf propeller, in addition to establishing the theoretically ideal propeller for this application. The propeller selection tool itself is based on the operating data of numerous off the shelf propellers and motors, which have in turn been processed in such a way that optimal combinations can be automatically established under given operating conditions. The outputs from the selection tool have also been compared to those obtained from a number of different validation methods in order to determine their accuracy. The results ultimately indicated that the “7x5” propeller was the most suitable off-the-shelf component for the case study, achieving remarkably similar performance to that of the theoretically ideal propeller for the application. Although the chosen validation methods essentially exposed the questionable accuracy of the tool in its current form, this study clearly concludes that the errors do not lie so much within the methods of the tool itself, but rather within the propeller and motor data on which it is based. Therefore, input data of greater accuracy would result in a tool which could be considered fit for purpose in its intended role.

**Keywords:** model aircraft, propeller, theoretical modelling, electrical efficiency, mechanical efficiency, motor, off-the-shelf, engineering.

## Introduction

Due to the current limitations of battery technology, improving the flight times of electric radio-controlled aircraft remains a challenge, especially for those who construct their own models (Avanzini, de Angelis & Giulietti, 2016). Logically, the flight duration depends largely on the batteries discharge rate, and thus the efficiency of the aircraft's propulsion system (Merchant, 2005).

Propulsion efficiency can be split into two components; The electrical efficiency and the mechanical efficiency. Electrical, or motor efficiency, $\eta_m$ (actually a combination of the motor and electronic speed controller (ESC) efficiencies in this case) is basically a measure of how well the battery power is converted into useful shaft power. Mechanical efficiency, on the other hand, is a measure of how well that shaft power is converted into a propulsive force (thrust) and depends almost entirely on the aircraft's propeller. Therefore, it can be called the "propeller efficiency", $\eta_p$, which is strongly dependant on the conditions in which the propeller is operating and how well it is matched to its powerplant.

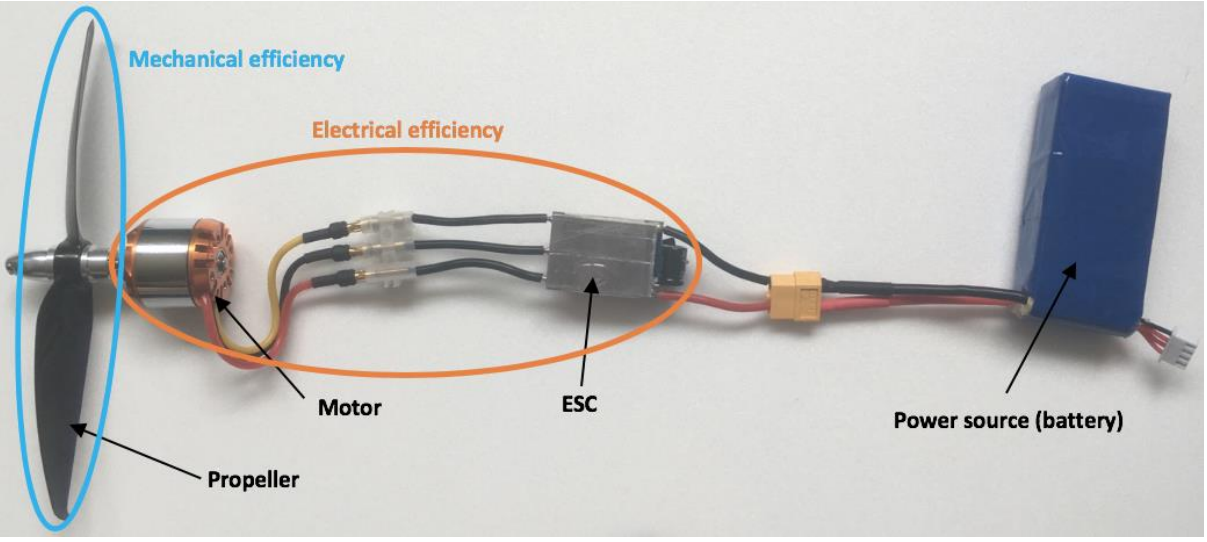


**Figure 1:** Model aircraft Propulsion system components

Matching the propeller to its powerplant is normally done through the comparison of propeller and motor data, which is not a problem for conventional aircraft where such data for both components has been widely charted and catalogued. Model aircraft, however, generally lack this, resulting in many broad assumptions and much speculation (Merchant, 2005). Furthermore, whilst electric motors are indeed often accompanied by a range of recommended propellers, selecting the ideal one for the intended operating conditions is rather hit and miss. This is problematic, as when attempting to maximise flight duration, finding the most appropriate propeller can make all the difference (Brandt & Selig, 2011). To summarise, current methods of matching propeller and motor for models are somewhat ambiguous, and although there is indeed some propeller and motor data available in the public domain, selecting the most suitable propeller remains a complicated task.

## Aims of this paper

1. To produce a mathematical Propeller selection model (PSM) capable of accurately determining the most suitable model aircraft propeller for a given application.
2. To establish the most suitable off-the-shelf propeller for the specified case study (see Table 1) such that; maximum propulsion efficiency is achieved under given cruise speed and thrust requirements.
3. To design, fabricate and test the theoretically most ideal propeller for the specified case study and compare to the “off-the -shelf” propeller deemed to be the most suitable by the PSM.

## Review of literature

This literature review has been approached from three directions; fundamental propeller theory; theory relevant to the PSM; and validation methods used.

### Fundamental propeller theory

*Basic concept*
The fundamental purpose of a propeller is to convert the supplied shaft power into useful thrust, and it achieves this by accelerating air mass to a higher velocity (Kane, 2020). A propeller can be considered as a set of aerofoils rotating around a central axis, where each foil represents an individual propeller blade. Each one of these “wings” is set at an angle from the plane of rotation, i.e. the propeller’s pitch angle, which directs airflow backwards. The resultant force on the propeller blades is known as the propeller’s thrust, *T*.

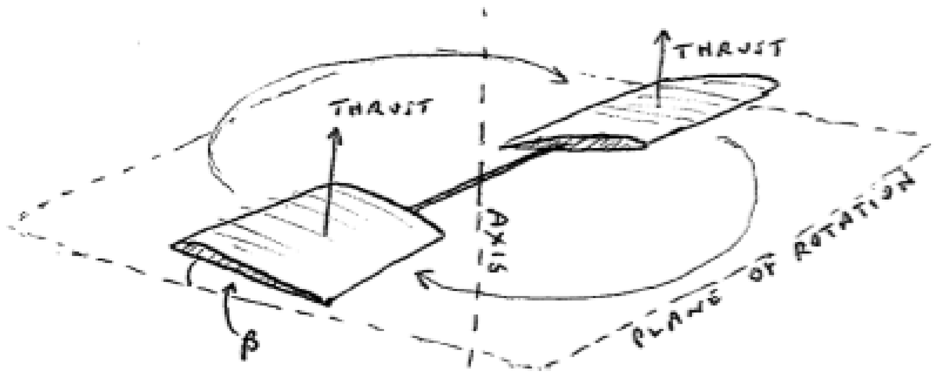


**Figure 2:** Propeller as a set of aerofoils

*Propeller Anatomy and design considerations*

There are 3 primary components to any propeller; The diameter, the number of blades, and the pitch.

<u>Diameter, D</u>
For efficiency, a large diameter is desirable. Nevertheless, limitations such as ground clearance and manufacture constraints need to be taken into consideration and mean that the theoretically most efficient propeller cannot always be used in practice (Kane, 2020).

Number of Blades, B

The number of blades affect the propeller's ability to "grab" the air, and thus, the total propeller thrust increases with their quantity. However, a greater number, among other things, increases the propeller's overall drag. Therefore, minimising the number of blades will maximise the potential for high $\eta_p$ (Gerr, 2001).

Pitch

Blade pitch greatly influences the propeller's speed of advance. In practice, most fixed pitch propellers have 2 forms of pitch; Rated pitch, which is the official pitch of the propeller measured at 75% of the blade radius (location of greatest thrust influence) (Garner, 2009), and; True geometric pitch ($\beta$), primarily used during design (Simons, 1999).

The relative airflow velocity, $W$, experienced by the blade is a vector composed of an axial velocity component due to airspeed, $V_a$, and a perpendicular velocity component, $\omega r$, due to blade rotation. The magnitude of each of these components will ultimately influence the relative flow angle, ø, on which the effective angle of attack, $\alpha$, is dependent. Note: a greater $V_a$ will reduce $\alpha$ and hence the rate of advance.

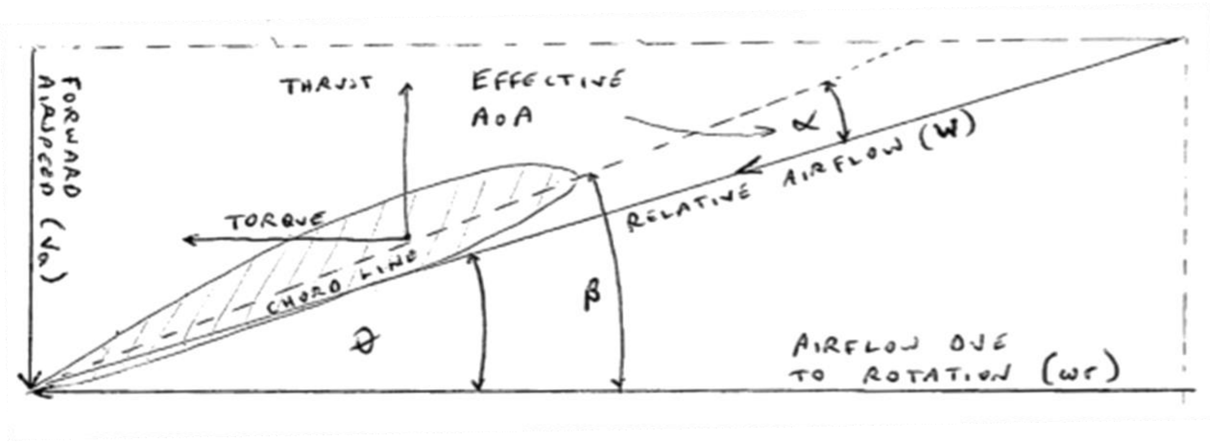


**Figure 3:** Angle of attack and velocity components

Since each section of the propeller blade has a greater perpendicular velocity component with increasing radial position, and thus a greater $\alpha$, $\beta$ typically decreases towards the tip of the blade, creating the distinct "twist" (Hitchens, 2015). This ensures that $\alpha$ remains relatively constant across each blade, improving efficiency (Weick, 1930). All things considered, most propellers are in fact not of this "constant $\alpha$" type, since they only operate efficiently at their intended *rpm* and airspeed, whilst performing considerably worse, or even unsatisfactorily, under all other conditions (e.g. at take-off). Slightly modifying the "twist" across the blade means that it will still perform very well under the intended conditions without underperforming in other regions of operation (Simons, 1999).

The optimum "minimum induced loss" propeller and propeller efficiency

Regarding propeller efficiency itself, Betz' theory on the "optimum propeller" shows that induced power losses (i.e. loss of propeller energy) are minimised if the axial velocity of the propeller's slipstream remains constant across the entire length of the blade (Eppler & Hepperle, 1984), ratifying the former claim that a constant $\alpha$ improves efficiency. In addition to the previously mentioned reduction in $\beta$ towards the tip, this can also be achieved in part by implementing an "elliptical chord distribution" along the blade (Simons, 1999).

Torque and propeller drag

During operation, each blade produces a drag force which attempts to resist the rotation of the propeller, otherwise known as the propeller's torque, *Q*, and it directly influences the shaft power requirements of the propeller. Keeping propeller pitch low significantly reduces the effect of torque, and pairing this with smooth, narrow blades (and thus a low Reynolds number) lowers drag and boosts propulsion efficiency (Simons, 1999).

## Research for producing the propeller selection model

*Propeller/motor specifications:*

Propeller rated properties

Most model propellers are accompanied by a number in the form of $\boldsymbol{X} \times \boldsymbol{Y}$ , which represents the $\boldsymbol{diamter} \times \boldsymbol{pitch}$ of the propeller. These "rated properties" are normally measured in inches, where the pitch is expressed as the theoretical distance the propeller would travel forwards in one full rotation (Weakley, 2018).

Pitch to diameter ratios

Propellers with differing pitch and diameter properties can be quickly compared dimensionlessly through their respective pitch/diameter (*P/D*) ratios.

Propeller advance ratios

Propeller Advance ratio, *J*, is essentially a ratio of how far the propeller travels forwards through the air in relation to its rate of rotation. Since it considers forwards velocity, $V_a$, it can also be considered a measure of the propeller's "dynamic efficiency" (Martinez, 2009).

$$J = \frac{v_a}{nD}$$ (Gur & Rosen, 2005)

**Equation 1**: Advance Ratio

Electric motor efficiency

Brushless motors frequently used in modelling lose a small portion of their energy through their windings and through mechanical friction at their shaft. Their efficiency can most easily be worked out using:

$$\eta_m = \frac{P_{shaft}}{P_{in}} \times 100$$ (Gabriel, Meyer & Du Plessis, 2011)

**Equation 2**: Brushless motor efficiency

Where…

$$P_{shaft} = \frac{2\pi \times rpm \times Q}{60}$$ (Purushothama Raj & Ramasamy, 2012)

**Equation 3**: Shaft power

*Propeller and motor curves*

Propeller and motor curves are a means of analysing how their individual properties, such as $\eta_m$ or $\eta_p$, vary with respect to another, e.g. *rpm*. However, these curves are also useful for analysing propeller and motor combinations. In this case, these combinations can be found through matching their torsional characteristics, as torque is the only propeller property the motor will actually "experience". This relationship is especially relevant to this paper, as the torque directly influences the motors power consumption and efficiency (Drela, 2005b).

Looking at an example of this relationship in Figure 4, it is important to note that both components will only operate in areas of torque "equilibrium", i.e. the points at which the propeller and motor curves intersect. For simplicity, this diagram only includes a single curve from each component, when in practice there would be many, many more. A well-matched propulsion system has so called "good impedance" when operating in a torque range corresponding to the peak efficiency of each component respectively (Drela, 2005b).

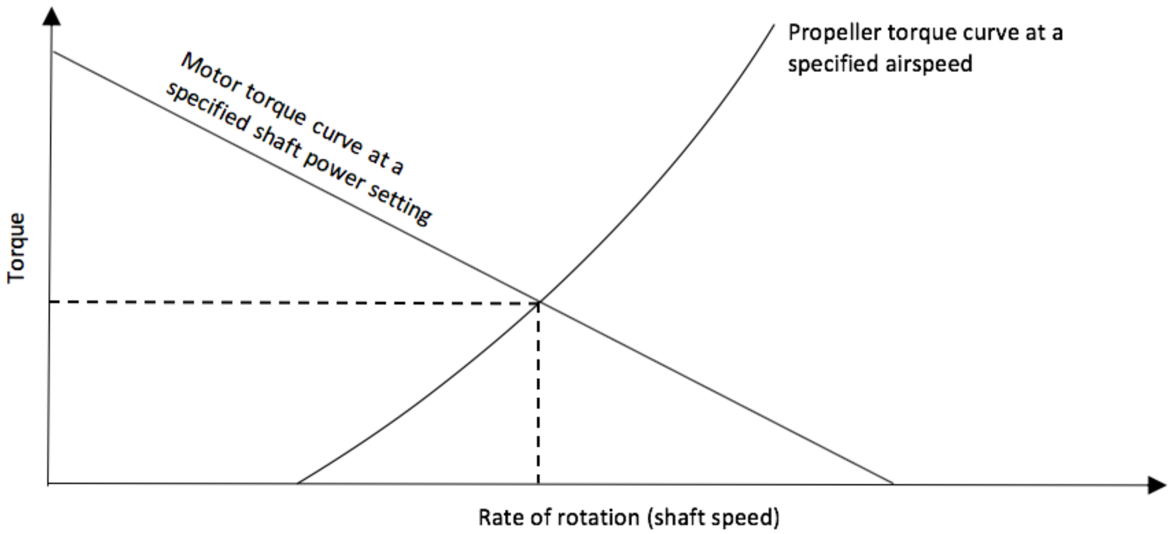


**Figure 4:** Propeller & motor torque curves

*Thrust requirements of case study*

In order to sustain flight at the given cruise speed, the thrust created by the propeller needs to match the airframe drag force, $F_D$, where:

$$T \geq F_D = \frac{1}{2} \times \rho \times C_D \times S \times {V_a}^2 \qquad \text{(Sherry \& Neyshabouri, 2014)}$$

**Equation 4:** Required thrust

The selected propeller must also be capable of providing take-off thrust requirements to overcome $F_D$ in addition to the aircrafts weight component due to the angle of climb, *Y*.

$$T > F_D + mgsin(\gamma) \qquad \text{(Sherry \& Neyshabouri, 2014)}$$

**Equation 5:** Take-off Thrust

The figures obtained as a result of the application of these equations can be viewed in Table 1.

**Background Research into the Validation methods used**
To check that the PSM is producing meaningful results, values for thrust should also be obtained by other means for direct comparison. Whilst research was originally done into numerous different validation methods, this section will only discuss the experimental and computational/theoretical methods which were used in full. Consideration was taken to ensure that these methods were fundamentally different from one another, as to avoid potentially suffering from the same drawbacks.

*Experimental validation methods and important considerations:*

Experimental method
Experimental methods of triangulation in this paper should occur through data obtained from the university wind tunnel. Various propeller types can be fitted to a test rig and thrust readings taken under the same operating conditions as those used in the PSM. Comparisons between results should then be made and conclusions drawn.

Propeller test rig
To meet the requirements of the test, the test rig should be able to measure thrust as a force and rate of propeller rotation in *rpm*. Torque readings would also be desirable as an additional form of test result validation (Kyte, 2020). Certain wind tunnel corrections may also need to be considered, not only for rectifying experimental data, but also for influencing the rig design. Solid blockage due to the size of the rig needs to be considered, where keeping the rig as slim as possible will reduce the need for any solid blockage corrections (Bass, 1986). Certain boundary corrections may also to be made, primarily "Glauert's correction", which considers how the difference between the tunnels jet velocity and the propeller's slipstream velocity influences the thrust of the propeller.

$$\frac{V'}{V_a} = 1 - \frac{\tau_4 \alpha}{2\sqrt{1+2\tau_4}} \quad \text{(Fitzgerald, 2007)}$$

**Equation 6**: Glauerts wind tunnel correction

Under experimental conditions of positive thrust, the slipstream velocity of the propeller is greater than the velocity of the wind tunnel jet ($V_a$) prior to the propeller disk. However, since the volume flow rate of the air must remain constant either side of the propeller disk, this means that the jet surrounding the propellers slipstream must have a reduced velocity ($w$) which is even lower than the $V_a$. This only occurs due to the walls of the test section, where in free air $w$ would of course be equal to $V_a$. Either way, due to this reduced jet velocity of $w$, there is consequently an increase in static pressure. Glauert proves that this increase in static pressure also causes an equal increase of static pressure within the propellers slipstream. This increase "reacts back to the propeller", such that the propeller produces an additional increment of thrust which would be equal to the thrust produced in a free air flow of velocity V'. V' is of course lower than $V_a$ (Fitzgerald, 2007). To summarise, Glauerts wind tunnel correction calculates a suitable velocity increment to add to the wind tunnel jet velocity $V_a$ in order to rectify the operating conditions.

It is also recommended that the propeller size is kept "small" (within 10% of wind tunnel area) (Barlow, Rae & Pope, 1999). Wake blockage is especially important as any objects behind the propeller disk have the potential to distort the thrust readings

(Kyte, 2019) especially if they are within the range of the propeller tips. Therefore, keeping the rig slim and aerodynamic is vital, as to minimize airflow distortion.

*Computational/theoretical validation methods*
The chosen computational validation tool “JavaProp” is a virtual propeller design and analysis tool. Developed by Martin Hepperle, it functions using the principles of blade element theory, meaning that it breaks each propeller blade down into a finite number of sections for design and analyses. Whilst JavaProp also takes the “optimum propeller” i.e. minimum induced loss concept into account, it does not consider 3D effects such as cross flow and flow separation (Hepperle, 2010).

This method was chosen for its simplicity of use, its ability to analyse multiple propeller properties simultaneously, and its ability to easily export propeller geometry.

## Investigation and discussion

Numerous investigations were completed in the attempt to satisfy the objectives of this paper, and as such, elements of the investigation and discussion have been placed alongside one another for clarity.

### Methodology summary

The investigation/discussion section will begin by outlining the case study operating parameters and hardware used for testing and validating the PSM. Subsequently, the PSM itself will be described in detail, including the origins of its operating principles and their significance. After this, the various validation procedures for examining the accuracy of the PSM will be discussed, followed by a complete comparison of all the results obtained.

### Case study operating parameters

The following parameters have been defined in order to test the excel model under “realistic” operating conditions, whilst also adhering to the limitations of the physical testing apparatus available for validation purposes:

**Table 1:** Case study Parameters

| Parameter | Value | Reason for choice |
|---|---|---|
| Model aircraft configuration | Flying wing | Minimum aerodynamic drag = greater flight duration. |
| Maximum propeller size | <7 inch (178mm) | Must be less than 10% of wind tunnel’s test section cross-sectional area. |
| Mass of model | Approx. 800g | Maximum realistic mass for a model possessing a 7-inch prop. |
| Wingspan of flying wing | Approx. 1500mm | Maximum realistic wingspan for model of this mass. |
| Estimated cruise speed | 15 m/s | Wind tunnels maximum speed is 16 m/s. |
| Estimated drag | 1N | $F_D = \frac{1}{2} \times \rho \times C_D \times S \times V_a^{2}$ (see lit review) |
| Required cruise thrust | ≥1N | Must be equal to airframe drag at cruise speed. |
| Required take-off thrust | ≥3.9N | $T > F_D + mgsin(\gamma)$ (see lit review) |

Please note: as a case study, these parameters are not overly precise or fully justified since they are solely required for providing a theoretical environment in which to test the PSM.

**Figure 5:** Flying wing model similar to the one described in Table 1

**Hardware selected for use in the propeller selection model**
The following propellers were chosen for use within the PSM based on a broad range of *P/D* ratios without breaching the wind tunnel restrictions. Care was also taken to ensure that at least half of these propellers were physically available for experimental validation.

**Table 2:** List of chosen propellers

| Propeller rated properties | Pitch to diameter ratio | Available for physical testing? |
|---|---|---|
| 5x3 | 0.60 | Yes |
| 5x4 | 0.80 | Yes |
| 6x2 | 0.33 | No |
| 6x3 | 0.50 | Yes |
| 6x4.5 | 0.75 | No |
| 7x3 | 0.43 | Yes |
| 7x4 | 0.57 | No |
| 7x5 | 0.71 | Yes |

The Vspec 2205 brushless motor was chosen as it was available and was also capable of achieving high *rpm*s (especially applicable for small, low pitch propellers).

**Propeller selection model and background theory**
This section describes the final version of the PSM. The various elements which have been critical for its creation will subsequently be described in detail.


**Figure 6:** Vspec 2205 2350kv 420W brushless motor

*Propeller Selection Model spreadsheet*

The PSM was produced entirely within a spreadsheet. Its layout can be viewed in Figure 7.

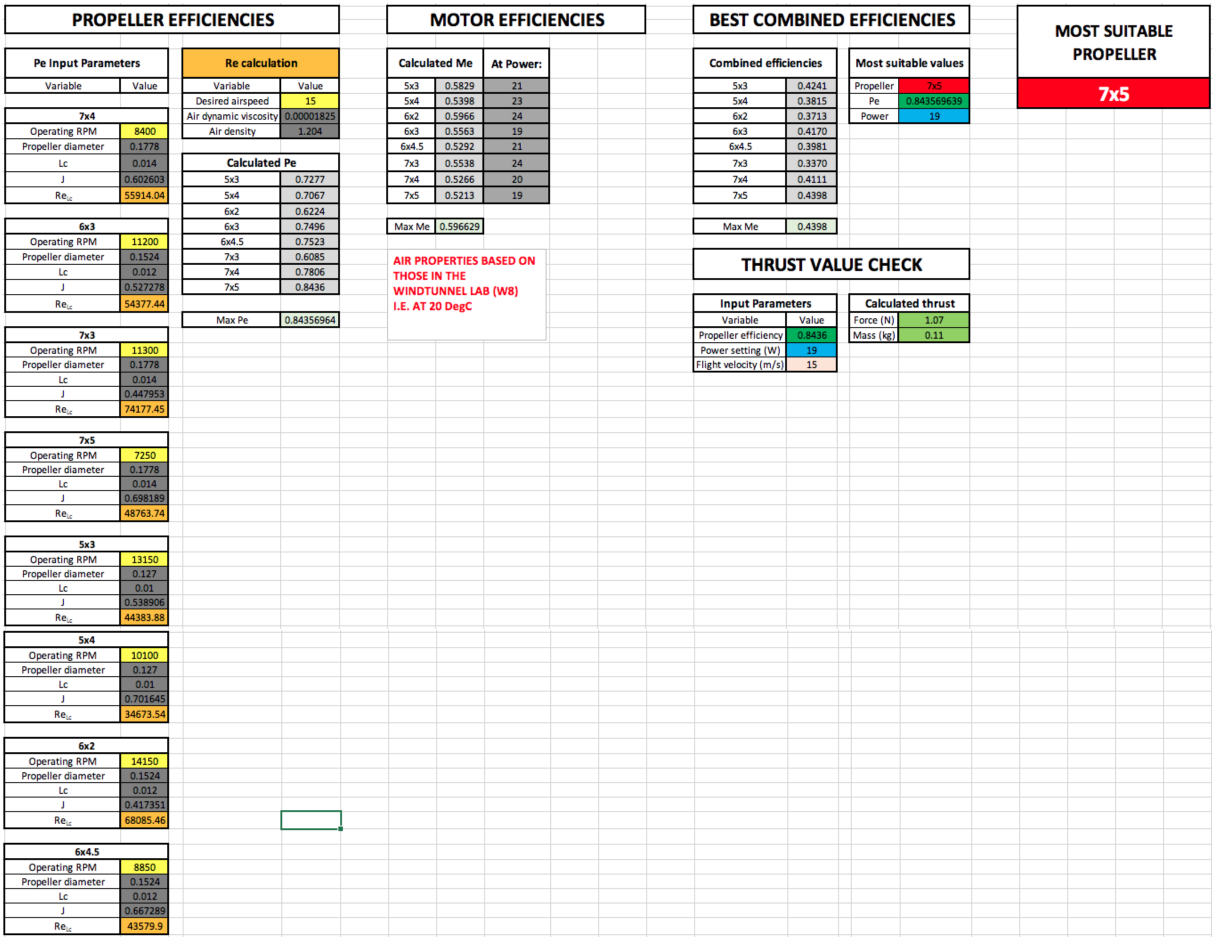

**PROPELLER EFFICIENCIES**

| Pe Input Parameters | |
|---|---|
| Variable | Value |
| **7x4** | |
| Operating RPM | 8400 |
| Propeller diameter | 0.1778 |
| Lc | 0.014 |
| J | 0.602603 |
| $Re_{Lc}$ | 55914.04 |
| **6x3** | |
| Operating RPM | 11200 |
| Propeller diameter | 0.1524 |
| Lc | 0.012 |
| J | 0.527278 |
| $Re_{Lc}$ | 54377.44 |
| **7x3** | |
| Operating RPM | 11300 |
| Propeller diameter | 0.1778 |
| Lc | 0.014 |
| J | 0.447953 |
| $Re_{Lc}$ | 74177.45 |
| **7x5** | |
| Operating RPM | 7250 |
| Propeller diameter | 0.1778 |
| Lc | 0.014 |
| J | 0.698189 |
| $Re_{Lc}$ | 48763.74 |
| **5x3** | |
| Operating RPM | 13150 |
| Propeller diameter | 0.127 |
| Lc | 0.01 |
| J | 0.538906 |
| $Re_{Lc}$ | 44383.88 |
| **5x4** | |
| Operating RPM | 10100 |
| Propeller diameter | 0.127 |
| Lc | 0.01 |
| J | 0.701645 |
| $Re_{Lc}$ | 34673.54 |
| **6x2** | |
| Operating RPM | 14150 |
| Propeller diameter | 0.1524 |
| Lc | 0.012 |
| J | 0.417351 |
| $Re_{Lc}$ | 68085.46 |
| **6x4.5** | |
| Operating RPM | 8850 |
| Propeller diameter | 0.1524 |
| Lc | 0.012 |
| J | 0.667289 |
| $Re_{Lc}$ | 43579.9 |

| Re calculation | |
|---|---|
| Variable | Value |
| Desired airspeed | 15 |
| Air dynamic viscosity | 0.00001825 |
| Air density | 1.204 |

| Calculated Pe | |
|---|---|
| 5x3 | 0.7277 |
| 5x4 | 0.7067 |
| 6x2 | 0.6224 |
| 6x3 | 0.7496 |
| 6x4.5 | 0.7523 |
| 7x3 | 0.6085 |
| 7x4 | 0.7806 |
| 7x5 | 0.8436 |
| Max Pe | 0.84356964 |

**MOTOR EFFICIENCIES**

| Calculated Me | | At Power: |
|---|---|---|
| 5x3 | 0.5829 | 21 |
| 5x4 | 0.5398 | 23 |
| 6x2 | 0.5966 | 24 |
| 6x3 | 0.5563 | 19 |
| 6x4.5 | 0.5292 | 21 |
| 7x3 | 0.5538 | 24 |
| 7x4 | 0.5266 | 20 |
| 7x5 | 0.5213 | 19 |
| Max Me | 0.596629 | |

AIR PROPERTIES BASED ON THOSE IN THE WINDTUNNEL LAB (W8) I.E. AT 20 DegC

**BEST COMBINED EFFICIENCIES**

| Combined efficiencies | |
|---|---|
| 5x3 | 0.4241 |
| 5x4 | 0.3815 |
| 6x2 | 0.3713 |
| 6x3 | 0.4170 |
| 6x4.5 | 0.3981 |
| 7x3 | 0.3370 |
| 7x4 | 0.4111 |
| 7x5 | 0.4398 |
| Max Me | 0.4398 |

| Most suitable values | |
|---|---|
| Propeller | 7x5 |
| Pe | 0.843569639 |
| Power | 19 |

**THRUST VALUE CHECK**

| Input Parameters | |
|---|---|
| Variable | Value |
| Propeller efficiency | 0.8436 |
| Power setting (W) | 19 |
| Flight velocity (m/s) | 15 |

| Calculated thrust | |
|---|---|
| Force (N) | 1.07 |
| Mass (kg) | 0.11 |

**MOST SUITABLE PROPELLER**

**7x5**

**Figure 7:** Propeller selection model spreadsheet layout

The PSM is divided into 5 primary sections: Propeller efficiencies (including the relevant input variables for each propeller down the left); motor efficiencies; combined efficiencies; thrust check; and final propeller selection.

Function

The primary function of this PSM is to determine the most suitable model aircraft propeller for a given application, just as stated in the aims. In this case, it has been tailored to meet the requirements of the case study – i.e. to identify the most suitable off-the-shelf propeller for maximising the propulsion efficiency and hence the flight duration of the theoretical model aircraft. This PSM relies on the use of raw propeller and motor operating data.

Basic operating principles

The PSM essentially determines propeller and motor combinations with the greatest combined propeller and motor efficiencies from the given data and operating conditions. The model's basic working principles begin by obtaining the *rpm* at which each propeller must operate in order to produce the desired amount of thrust at a specified air speed. It does this through the raw propeller data. Using just this value for *rpm* as an input variable together with the desired airspeed (both shown in yellow for each propeller), intermediate properties are then calculated. Among others, these include the advance ratio and rated-chord-based Reynolds number, $Re_{Lc}$, of each propeller, the torque acting on the prop shaft, and the required shaft power, $P_{shaft}$, from the motor. These intermediate properties ultimately enable the calculation of the propeller and motor efficiencies, which are in turn multiplied to give an overall propulsion efficiency. These "combined efficiencies" are simply numerical ratings, the highest value of which will indicate which propeller is the most suitable for use. The "Thrust value check" section of the model confirms that the selected propeller does indeed meet its intended thrust requirements, and does so through the use of:

$$T = \frac{\eta_p \times P_{shaft}}{V_a}$$ (Gerr, 2001)

**Equation 7**: Propeller thrust as a function of propeller efficiency

Although in its final form the PSM processes this information largely automatically from the input variables, for clarification, its operation has also been performed (in part) manually as demonstrated in "Operation principles and theory" under the "*Performance curves spreadsheet*" section below.

Features

One of the main features of the PSM is its use of 3D regressions for automating the calculations of the propeller and motor efficiencies using the previously mentioned intermediate properties. 3D regressions are needed as both efficiencies depend on more than just one variable. Whilst propeller efficiency relies on $J$ in addition to the respective $Re_{Lc}$, motor efficiency is proportional to *rpm* as well as the motors shaft power. Both regressions are third order and were obtained using IBM's SPSS statistical analysis software. Whilst the regression for $\eta_p$ was found relatively easily using the raw propeller data from the "Performance curves" spreadsheet (see below), the data for the $\eta_m$ regression was obtained experimentally, as described in "Experimental motor data" section. An example of one of these 3D surface plots can be viewed in Figure 8.

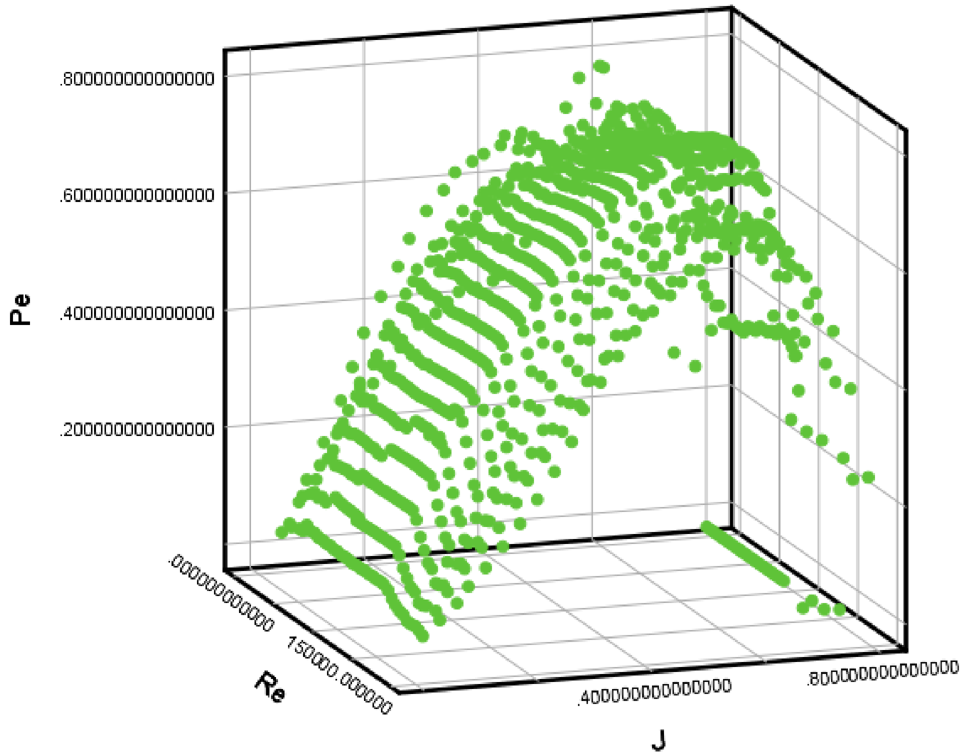


**Figure 8:** Propeller efficiency surface plot, including Reynolds number and Advance ratio on the 2 opposing axes

Results – propeller deemed the most suitable by the PSM

As seen in Figure 9, the PSM has concluded that the 7x5 is the most suitable propeller for the case study application, sporting the largest combined efficiency rating of 43.98. Furthermore, the thrust check confirms that the 7x5 does indeed meet the thrust requirement of 1N. Its required shaft power is 19W.

**BEST COMBINED EFFICIENCIES**

| Combined efficiencies | |
|---|---|
| 5x3 | 0.4241 |
| 5x4 | 0.3815 |
| 6x2 | 0.3713 |
| 6x3 | 0.4170 |
| 6x4.5 | 0.3981 |
| 7x3 | 0.3370 |
| 7x4 | 0.4111 |
| 7x5 | 0.4398 |
| Max Me | 0.4398 |

| Most suitable values | |
|---|---|
| Propeller | 7x5 |
| Pe | 0.843569639 |
| Power | 19 |

**THRUST VALUE CHECK**

| Input Parameters | |
|---|---|
| Variable | Value |
| Propeller efficiency | 0.8436 |
| Power setting (W) | 19 |
| Flight velocity (m/s) | 15 |

| Calculated thrust | |
|---|---|
| Force (N) | 1.07 |
| Mass (kg) | 0.11 |

**Figure 9:** Propeller selection model case study results

Accuracy and limitations

Regarding the PSM's accuracy, the regressions for the efficiencies are essentially an expression of "best fit" and will work better for some propellers than others. Additionally, due to the large spread of input data from which the regressions were determined, their precision isn't necessarily the best, with the $\eta_m$ regression having a coefficient of determination ($R^2$) value of just 0.393, suggesting that a large amount of the variation within the data could not be accounted for. Finally, as a practical tool, one might also argue that the model's reliance on raw propeller operating data is in itself a limitation, as it will only ever be as accurate as this data. Theoretically, it would also require the operating data of every propeller in existence if it was to select the true, best propeller for the any desired application.

*"Performance curves" spreadsheet*

Purpose of spreadsheet

This spreadsheet essentially provided a starting point from which the PSM has grown. It not only contains the majority of the background theory used, but also serves as a sort of "bank" of all the propeller and motor data. In addition to providing information on the operation of the propellers and motors, it also provides the relevant data for the $\eta_p$ regression. In the context of this paper, this spreadsheet will assist in explaining some of the theory behind the operation of the PSM.

Primary features

All of the propeller data used in this spreadsheet was downloaded online from website "apcprop.com" (apcprop.com, 2019). It in turn uses the "NASA Transonic Airfoil Analysis Computer Program" to accurately obtain this data. A snippet of one of this spreadsheet's propeller data banks can be viewed below.

| DEFINITIONS: | | |
|---|---|---|
| J | V/nD | Advance Ratio |
| Ct | T/(ρ*n^2*D^4) | Thrust coefficient |
| Cp | P/(ρ*n^3*D^5) | Power coefficient |
| Pe | Ct*J/Cp | Propeller Efficiency |
| V | | Model speed (m/s) |
| n | | Rev per sec (1/s) |
| D | 0.1778 | Diameter (m) |
| ρ | 1.225 | Air density (kg/m^3) @15℃ |
| μ | 0.00001789 | Air dynamic viscosity (Pa.s) @15℃ |
| $C_Q$ | Q/(ρ*n^2*D^5) | Torque coefficient |
| $L_{c0.75}$ | 0.014 | Chord Length 0.75 Radius (m) |

| Useful conversions | | |
|---|---|---|
| Lbf to Newtons | * | 4.44822 |
| Hp to Watts | * | 745.7 |
| In-Lbf to Nm | * | 0.1129848 |
| mph to m/s | * | 0.44704 |

IMPORTANT NOTES!

Tip velocity is exceeding the speed of sound at higher RPMs. This will drastically affect the propellers efficiecy! (through transonic losses).

| V | J | Pe | Ct | Cp | $C_Q$ | PWR | Torque | Thrust | RPM | Prop Relative V [$V_p$] | $Re_{Lc}$ |
|---|---|---|---|---|---|---|---|---|---|---|---|
| (m/s) | (Advance Ratio) | | Calculated | | | W | Nm | N | 1/min | (m/s) | |
| 0 | 0.00 | 0 | 0.1145 | 0.09250 | 0.0088761 | 0.7457 | 0.0021467 | 0.1556877 | 2000 | 13.96437935 | 13386.76 |
| 0.178816 | 0.03 | 0.037333313 | 0.1145 | 0.0924981 | 0.0093432 | 0.7457 | 0.0022597 | 0.1556877 | 2000 | 13.96552418 | 13387.86 |
| 0.402336 | 0.07 | 0.083999955 | 0.1145 | 0.0924981 | 0.0093432 | 0.7457 | 0.0022597 | 0.1556877 | 2000 | 13.97017411 | 13392.31 |
| 0.581152 | 0.10 | 0.121333268 | 0.1145 | 0.0924981 | 0.0098104 | 0.7457 | 0.0023727 | 0.1556877 | 2000 | 13.97646694 | 13398.35 |
| 0.759968 | 0.13 | 0.158666582 | 0.1145 | 0.0924981 | 0.0098104 | 0.7457 | 0.0023727 | 0.1556877 | 2000 | 13.98504351 | 13406.57 |
| 0.983488 | 0.17 | 0.205333223 | 0.1145 | 0.0924981 | 0.0098104 | 0.7457 | 0.0023727 | 0.1556877 | 2000 | 13.99896922 | 13419.92 |
| 1.162304 | 0.20 | 0.242666537 | 0.1145 | 0.0924981 | 0.0102776 | 0.7457 | 0.0024857 | 0.1556877 | 2000 | 14.01266717 | 13433.05 |
| 1.34112 | 0.23 | 0.271999854 | 0.1112 | 0.0924981 | 0.0102776 | 0.7457 | 0.0024857 | 0.1512395 | 2000 | 14.0286312 | 13448.35 |
| 1.56464 | 0.26 | 0.317333163 | 0.1112 | 0.0924981 | 0.0102776 | 0.7457 | 0.0024857 | 0.1512395 | 2000 | 14.05176106 | 13470.53 |
| 1.743456 | 0.29 | 0.353599811 | 0.1112 | 0.0924981 | 0.0107447 | 0.7457 | 0.0025987 | 0.1512395 | 2000 | 14.07279394 | 13490.69 |
| 1.922272 | 0.32 | 0.378399797 | 0.1079 | 0.0924981 | 0.0107447 | 0.7457 | 0.0025987 | 0.1467913 | 2000 | 14.09606399 | 13513.00 |
| 2.145792 | 0.36 | 0.409599781 | 0.1046 | 0.0924981 | 0.0107447 | 0.7457 | 0.0025987 | 0.142343 | 2000 | 14.12828064 | 13543.88 |
| 2.324608 | 0.39 | 0.429866437 | 0.1014 | 0.0924981 | 0.0107447 | 0.7457 | 0.0025987 | 0.1378948 | 2000 | 14.1565424 | 13570.97 |
| 2.548128 | 0.43 | 0.455999756 | 0.0981 | 0.0924981 | 0.0107447 | 0.7457 | 0.0025987 | 0.1334466 | 2000 | 14.1949585 | 13607.80 |
| 2.726944 | 0.46 | 0.471733081 | 0.0948 | 0.0924981 | 0.0102776 | 0.7457 | 0.0024857 | 0.1289984 | 2000 | 14.22814514 | 13639.61 |
| 2.90576 | 0.49 | 0.467999749 | 0.0883 | 0.0924981 | 0.0102776 | 0.7457 | 0.0024857 | 0.1201019 | 2000 | 14.26349647 | 13673.50 |
| 3.12928 | 0.53 | 0.485333074 | 0.0850 | 0.0924981 | 0.0098104 | 0.7457 | 0.0023727 | 0.1156537 | 2000 | 14.31070522 | 13718.76 |
| 3.308096 | 0.56 | 0.473599746 | 0.0785 | 0.0924981 | 0.0093432 | 0.7457 | 0.0022597 | 0.1067573 | 2000 | 14.35086721 | 13757.26 |
| 3.486912 | 0.59 | 0.457599755 | 0.0719 | 0.0924981 | 0.0088761 | 0.7457 | 0.0021467 | 0.0978608 | 2000 | 14.39313884 | 13797.78 |
| 3.710432 | 0.63 | 0.44266643 | 0.0654 | 0.0924981 | 0.0084089 | 0.7457 | 0.0020337 | 0.0889644 | 2000 | 14.44891678 | 13851.25 |
| 3.889248 | 0.66 | 0.417599776 | 0.0589 | 0.0924981 | 0.0079418 | 0.7457 | 0.0019207 | 0.080068 | 2000 | 14.49586632 | 13896.26 |
| 4.068064 | 0.69 | 0.412533112 | 0.0556 | 0.0924981 | 0.0074746 | 0.7457 | 0.0018078 | 0.0756197 | 2000 | 14.54486285 | 13943.23 |
| 0 | 0.00 | 0 | 0.1148 | 0.0548137 | 0.0091356 | 1.4914 | 0.0049713 | 0.3514094 | 3000 | 20.94656902 | 20080.14 |
| 0.312928 | 0.04 | 0.073733294 | 0.1148 | 0.0548137 | 0.0093432 | 1.4914 | 0.0050843 | 0.3514094 | 3000 | 20.94890636 | 20082.38 |
| 0.581152 | 0.07 | 0.13693326 | 0.1148 | 0.0548137 | 0.0095509 | 1.4914 | 0.0051973 | 0.3514094 | 3000 | 20.95462935 | 20087.86 |
| 0.89408 | 0.10 | 0.210666554 | 0.1148 | 0.0548137 | 0.0095509 | 1.4914 | 0.0051973 | 0.3514094 | 3000 | 20.96564172 | 20098.42 |
| 1.162304 | 0.13 | 0.27386652 | 0.1148 | 0.0548137 | 0.0097585 | 1.4914 | 0.0053103 | 0.3514094 | 3000 | 20.97879177 | 20111.03 |
| 1.475232 | 0.17 | 0.347599814 | 0.1148 | 0.0548137 | 0.0099661 | 1.4914 | 0.0054233 | 0.3514094 | 3000 | 20.99845383 | 20129.88 |
| 1.743456 | 0.20 | 0.405599783 | 0.1134 | 0.0548137 | 0.0101738 | 1.4914 | 0.0055363 | 0.3469612 | 3000 | 21.01900075 | 20149.57 |
| 2.056384 | 0.23 | 0.478399744 | 0.1134 | 0.0548137 | 0.0103814 | 1.4914 | 0.0056492 | 0.3469612 | 3000 | 21.04726749 | 20176.67 |
| 2.324608 | 0.26 | 0.533866381 | 0.1119 | 0.0548137 | 0.0103814 | 1.4914 | 0.0056492 | 0.3425129 | 3000 | 21.07516444 | 20203.41 |
| 2.637536 | 0.30 | 0.597866347 | 0.1105 | 0.0548137 | 0.010589 | 1.4914 | 0.0057622 | 0.3380647 | 3000 | 21.11197172 | 20238.70 |

**Figure 10:** Propeller data bank example (after being converted to metric units)

One of the most important features of this spreadsheet is how it analyses the propellers and motor together as one propulsion system. It does so through the torque-rpm relationship mentioned in the literature review. Figure 11 illustrates this relationship, where each propeller curve is operating at the speed of 15 m/s and each motor curve represents a different shaft power setting. Each component can only operate with the other under the conditions at which their curves intersect (Drela, 2005b). Note that the data for the motor curves was obtained from its own respective table of theoretical operating statistics.

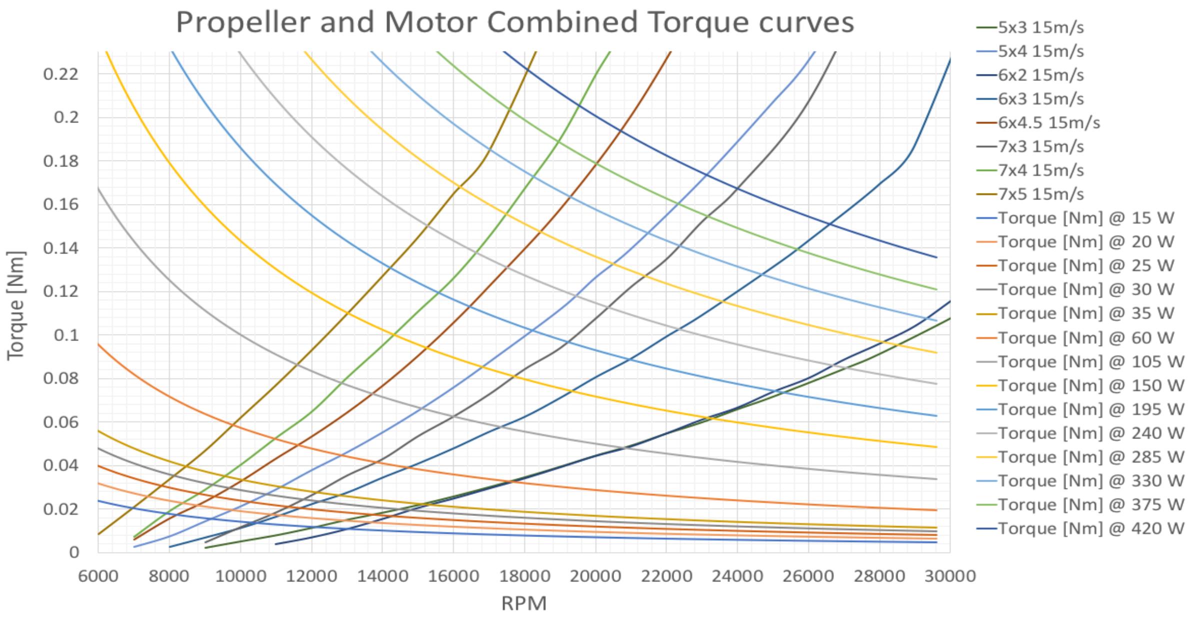


**Figure 11:** Propeller and motor torque curves

This relationship is directly used by the PSM, and essentially enables it to determine the required shaft power for each propeller at any *rpm*.

<u>Operation principles and theory</u>

As the PSM's theory is based on this spreadsheet, establishing the most suitable propeller can, in part, be performed manually here. This process is described in the flow chart below, where Figure 12 aids the description of step 1.

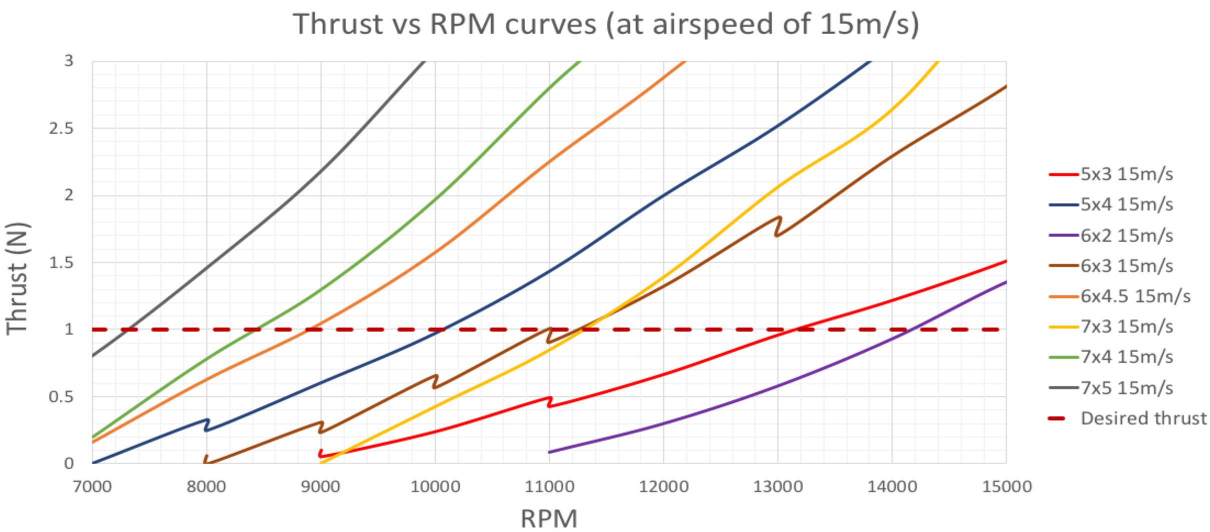


**Figure 12:** Propeller rpm at target thrust – constructed from the raw propeller data

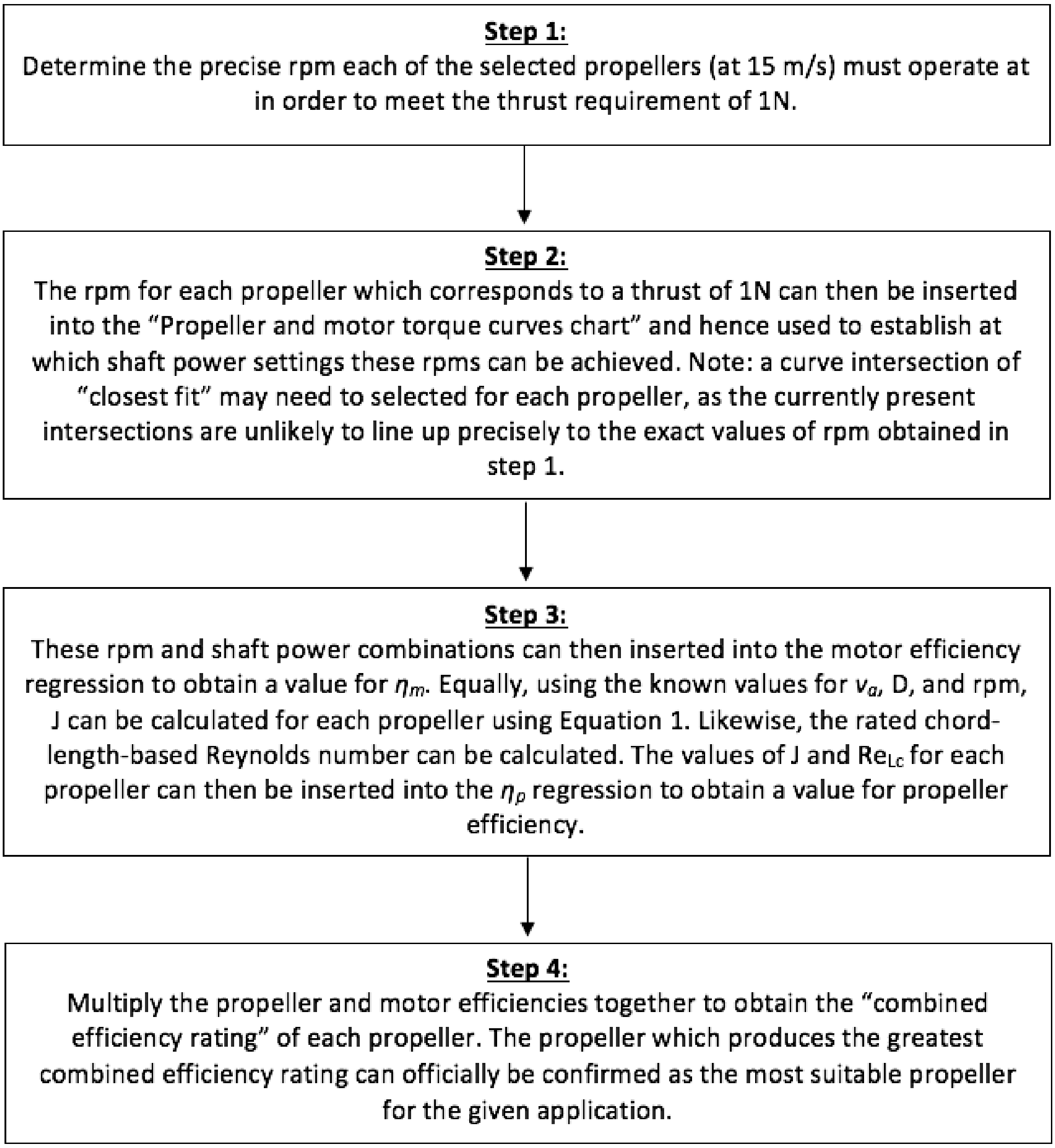


**Figure 13:** Propeller selection flow chart

### *Experimental motor data*

#### Purpose of the motor experiments

The purpose of these experiments was to produce a means of determining $\eta_m$ for use in the PSM's $\eta_m$ regression. Although these experiments were unable to measure $\eta_m$ from the selected motor directly, they were able to measure all the necessary variables for calculating $\eta_m$ later on.

#### Methodology and use of Experimental data

The simplest means of working out $\eta_m$ is by establishing how much of the input power is being converted into useful shaft power, as previously seen in Equation 2.

Equation 3 clearly indicates that the required shaft power is directly dependant on both the torque exerted by the propeller and the *rpm*. This means that altering these 2 variables independently of one another will essentially result in a 3D graph, or "surface plot" of shaft power. Since $\eta_m$ is directly proportional to the shaft power, the expected 3D $\eta_m$ chart should also feature a surface plot, very roughly illustrated for clarity in Figure 14.

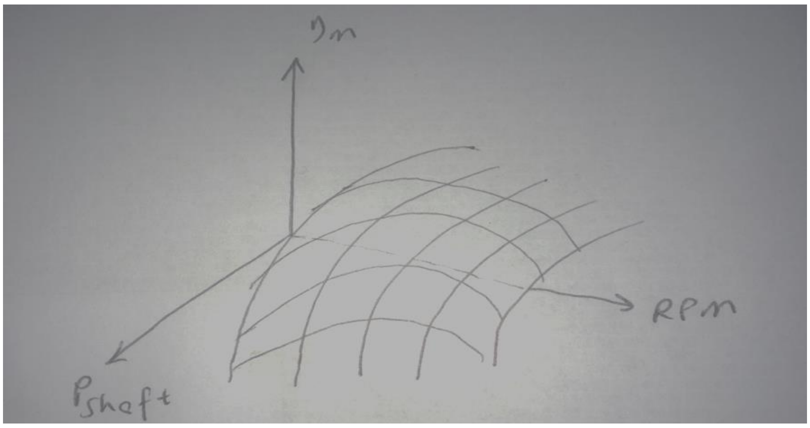


**Figure 14:** Motor Efficiency surface plot

The variables on which the $\eta_m$ regression depends are shaft power and *rpm*, as these are the most convenient variables for use within the PSM, and thus these are the primary variables that need to be obtained from the experiments.

Design

This rig was primarily designed around its ability to measure torque and *rpm* for use in Equation 3. Although several designs were constructed and tested, the final version measured torque through the use of a load cell, where propellers were used to apply the external torsional force. Note that multiple different propellers were used to ensure that *rpm* and torque were in essence varied independently of one another.

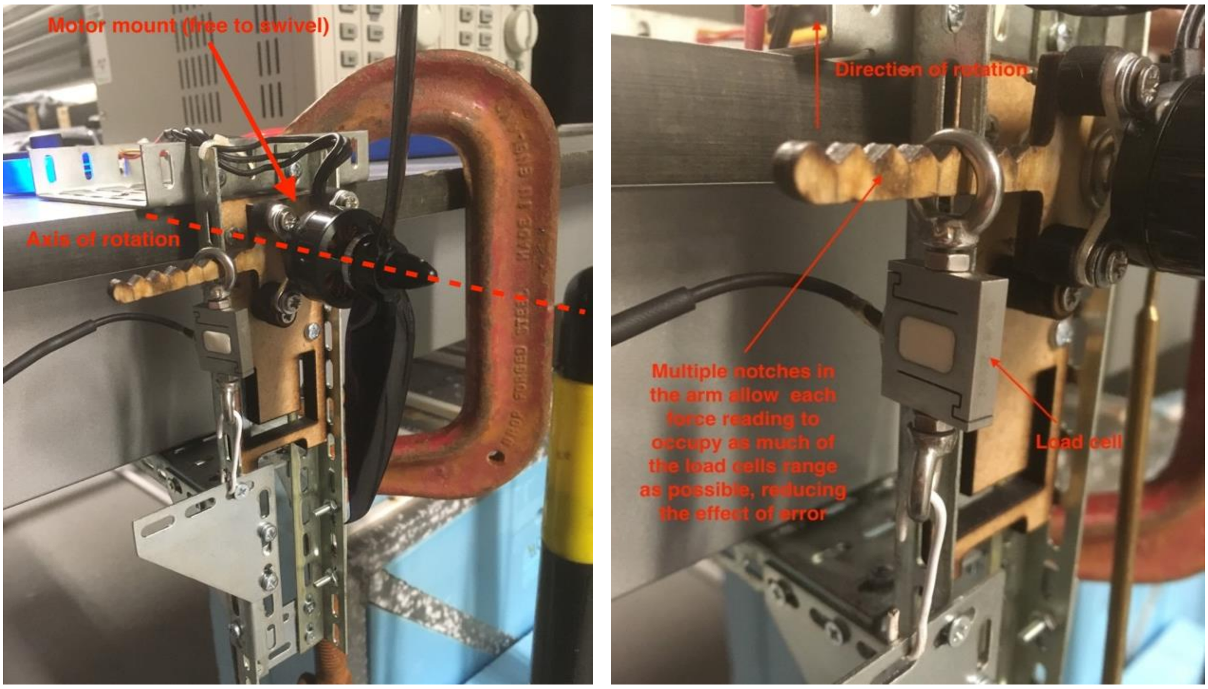


**Figure 15:** Torque test rig final revision

In response to the torque exerted on the motor, the plywood motor mount at the back was free to rotate and thus exert a force on the load cell. Multiplying this force by the load cells perpendicular distance to the axis of rotation would essentially provide the values for torque. $P_{in}$ was measured with a watt meter whilst *rpm* was measured using a laser tachometer.

Results

The experiment produced a considerable range of results, a snippet of which can be seen in Figure 16 (the first 3 columns are the direct experimental readings).

**Experimental results**

| Power (W) | Force (N) | RPM | Arm Distance (m) | Prop type | Torque (Nm) | Shaft Power (W) | Motor Efficiecy (%) | Motor Efficiecy (Reg.3rd order) (%) R^2=0.393 |
|---|---|---|---|---|---|---|---|---|
| 3.8 | 0.1 | 6000 | 0.027 | 6030 2B | 0.0027 | 1.696460033 | 44.64368508 | 54.02636337 |
| 9.9 | 0.175 | 9800 | 0.027 | 5030 2B | 0.004725 | 4.849048261 | 48.98028546 | 55.55816699 |
| 9.8 | 0.19 | 9000 | 0.027 | 5030 3B | 0.00513 | 4.834911094 | 49.33582749 | 54.79957747 |
| 5 | 0.2 | 5100 | 0.027 | 6045 2B | 0.0054 | 2.883982056 | 57.67964112 | 54.05918682 |
| 7.4 | 0.2 | 6800 | 0.027 | 7035 2B | 0.0054 | 3.845309408 | 51.96364065 | 53.74342535 |
| 8.6 | 0.2 | 8400 | 0.027 | 5040 2B | 0.0054 | 4.750088092 | 55.23358247 | 54.34576945 |
| 8.7 | 0.2 | 7900 | 0.027 | 5045 2B | 0.0054 | 4.467344753 | 51.34879027 | 54.07395525 |
| 13.5 | 0.22 | 9600 | 0.027 | 5040 2B | 0.00594 | 5.971539316 | 44.23362456 | 55.19404809 |
| 14.6 | 0.24 | 10000 | 0.027 | 5040 2B | 0.00648 | 6.785840132 | 46.47835707 | 55.49909005 |
| 9.9 | 0.25 | 7500 | 0.027 | 7035 2B | 0.00675 | 5.301437603 | 53.54987478 | 53.75482716 |
| 13.6 | 0.25 | 11100 | 0.027 | 5030 2B | 0.00675 | 7.846127652 | 57.69211509 | 56.67208123 |
| 18.5 | 0.275 | 12300 | 0.027 | 5030 2B | 0.007425 | 9.563793436 | 51.69618073 | 58.11927721 |
| 9.8 | 0.3 | 6200 | 0.027 | 6045 2B | 0.0081 | 5.259026102 | 53.66353165 | 53.47338648 |
| 10.9 | 0.3 | 7200 | 0.027 | 5045 3B | 0.0081 | 6.107256119 | 56.02987265 | 53.5251951 |
| 12.4 | 0.3 | 8000 | 0.027 | 5040 3B | 0.0081 | 6.785840132 | 54.72451719 | 53.80298605 |
| 14.5 | 0.3 | 10700 | 0.027 | 5030 3B | 0.0081 | 9.076061176 | 62.59352535 | 56.01168685 |
| 16.1 | 0.3 | 9400 | 0.027 | 5045 2B | 0.0081 | 7.973362155 | 49.52398854 | 54.72977284 |
| 23.2 | 0.32 | 13300 | 0.027 | 5030 2B | 0.00864 | 12.0335565 | 51.86877802 | 59.35453113 |
| 9.9 | 0.35 | 5600 | 0.027 | 5550 2B | 0.00945 | 5.541769441 | 55.9774691 | 53.50107672 |
| 16.3 | 0.35 | 9000 | 0.027 | 5040 3B | 0.00945 | 8.906415173 | 54.64058388 | 54.24956125 |
| 19.4 | 0.35 | 11100 | 0.027 | 5040 2B | 0.00945 | 10.98457871 | 56.62153976 | 56.28727945 |
| 11.6 | 0.4 | 6000 | 0.027 | 6042 2B | 0.0108 | 6.785840132 | 58.49862183 | 53.26841805 |
| 12.3 | 0.4 | 6900 | 0.027 | 6045 2B | 0.0108 | 7.803716152 | 63.44484676 | 53.20983847 |
| 15.6 | 0.4 | 8100 | 0.027 | 5045 3B | 0.0108 | 9.160884178 | 58.72361652 | 53.55519261 |
| 18.5 | 0.4 | 9300 | 0.027 | 7035 2B | 0.0108 | 10.5180522 | 56.85433624 | 54.32177605 |
| 20.4 | 0.4 | 11800 | 0.027 | 5030 3B | 0.0108 | 13.34548559 | 65.41904702 | 56.97259183 |
| 20.5 | 0.4 | 16300 | 0.027 | 4045 2B | 0.0108 | 18.43486569 | 89.9261741 | 63.62781443 |
| 25.2 | 0.4 | 12000 | 0.027 | 5040 2B | 0.0108 | 13.57168026 | 53.85587406 | 57.23227495 |
| 19.7 | 0.42 | 10300 | 0.027 | 6030 2B | 0.01134 | 12.23147684 | 62.08871491 | 55.16830085 |
| 27.6 | 0.42 | 13000 | 0.027 | 5030 3B | 0.01134 | 15.4377863 | 55.93400833 | 58.53511117 |
| 30.5 | 0.42 | 18800 | 0.027 | 4045 2B | 0.01134 | 22.32541403 | 73.1980788 | 67.19511805 |
| 36 | 0.42 | 15400 | 0.027 | 5030 2B | 0.01134 | 18.28783916 | 50.79955321 | 62.15714633 |
| 18.9 | 0.45 | 8800 | 0.027 | 5045 3B | 0.01215 | 11.19663622 | 59.24146147 | 53.80977605 |
| 30.9 | 0.45 | 13100 | 0.027 | 5040 2B | 0.01215 | 16.66771982 | 53.94084085 | 58.57396609 |
| 16 | 0.5 | 6500 | 0.027 | 5550 2B | 0.0135 | 9.189158512 | 57.4322407 | 52.96479803 |

**Figure 16:** Snippet of motor efficiency experimental results

The true, theoretical efficiencies (shown in green) were first calculated using the principles described in the "Methodology and use of Experimental data" section above. This column, together with the chosen motor variables (*rpm* and $P_{shaft}$ - shown in yellow) were subsequently used to produce the 3D regression on SPSS for finding $\eta_m$. The 3rd order regression (with $R^2 = 0.393$) produced the efficiency outputs shown in orange. As can be seen, whilst many of the efficiency values lie only within a few percent of those previously calculated (in green), others appear to differ considerably, by over 10% in places. This shows that whilst the results from this experiment might be workable, they are by no means very precise.

Experimental accuracy and limitations

The lack of any proper ball bearings within the rig assembly meant that the motor mount was only free to rotate around the bolt fastening it to the rest of the rig. This will have impacted accuracy, especially when measuring low amounts of torque, due to a portion of it being used to overcome the rotational friction.

Additionally, due to time constraints and rushed production, the motor mount was only supported at one end. This essential allowed the entire motor mount to "droop" somewhat, likely increasing its friction.

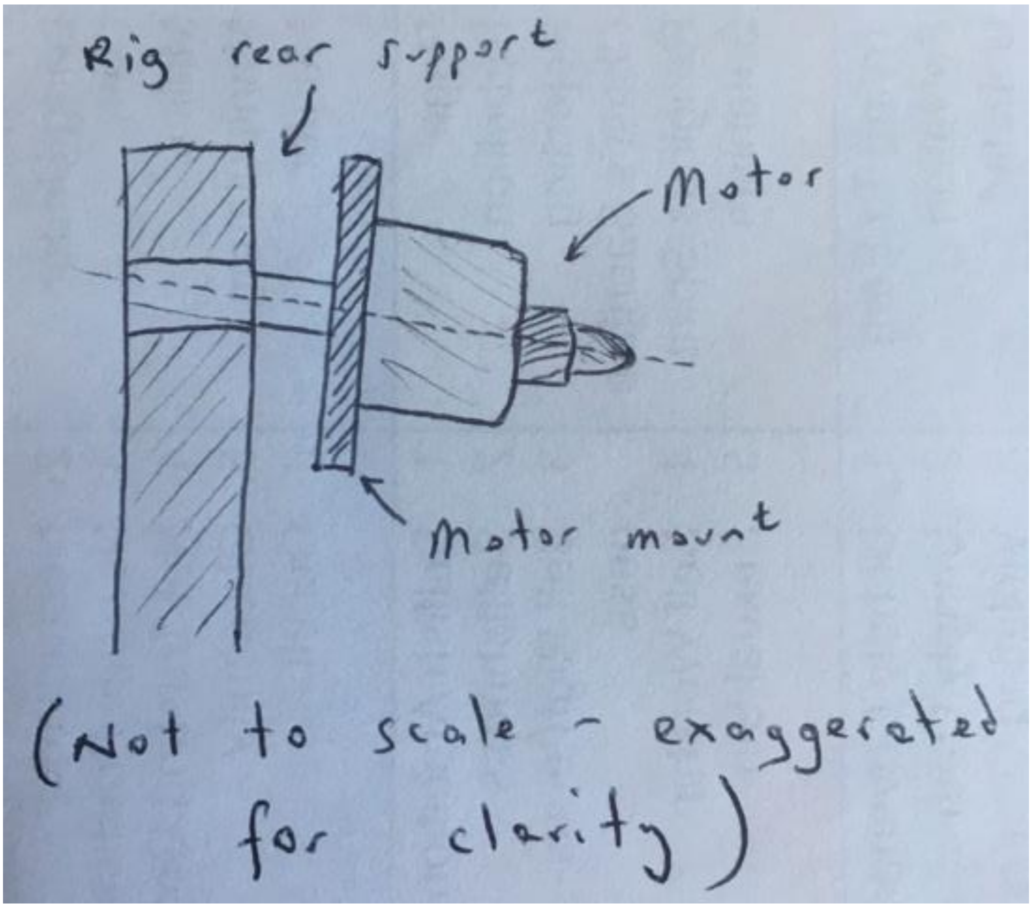


**Figure 17:** Torque rig "droop"

The measuring equipment used might also have contributed to inaccuracies in the results. The load cell, for example, whilst initially being well calibrated using known weights and zeroed out for the no-load case, appeared to be only accurate to at best ± 0.2N. This meant that at very low readings (as low as 0.1N), a sort of "average" value needed to be estimated from the output graph (Figure 18), which undoubtably had an impact on the results.


**Figure 18:** Load cell output reading

Note: The alignment of the load cell was not a concern here. A maximum displacement of 5° in 2 directions would only have meant a total error of 0.76%.

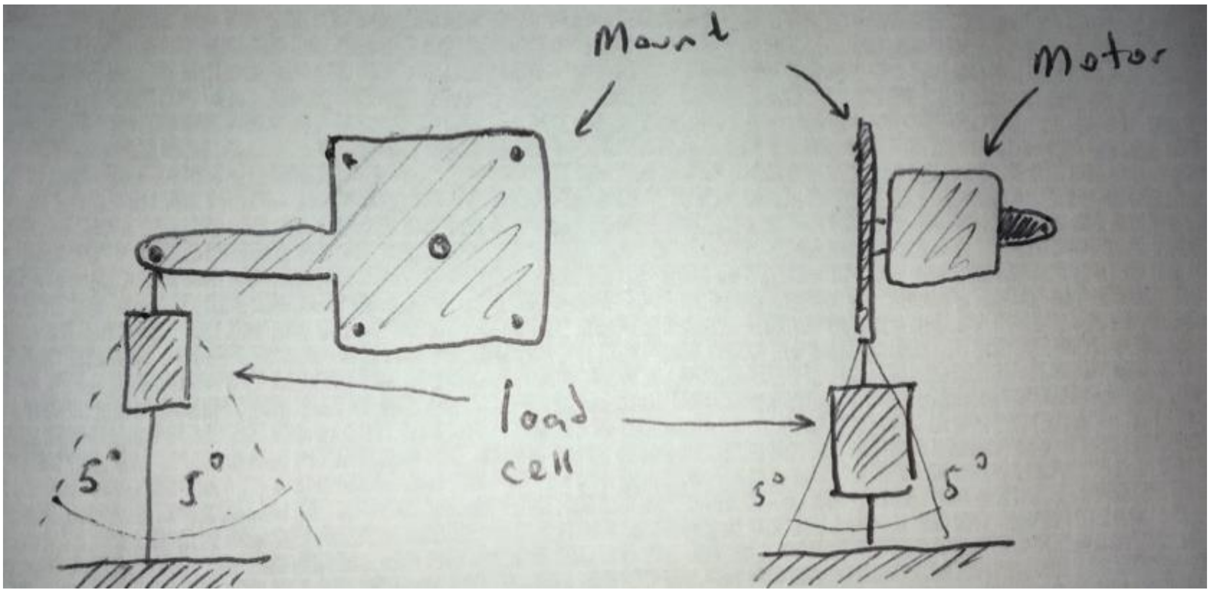


**Figure 19:** Load cell mounting accuracy

**Validating the outputs of the PSM**
Multiple validation methods were used to check whether the PSM was producing adequate results. To reiterate, these were; experimental methods using the wind tunnel; and computational/theoretical analysis methods using JavaProp. Note that the computational/theoretical methods were also used to design the theoretically ideal propeller for the case study using JavaProps "design" function.

*Wind tunnel experiments*

Aims
The aim of these experiments was simply to check that the calculated thrust produced by the propellers in the PSM was true to life. Ideally, they would also indicate the accuracy to which $\eta_p$ and $\eta_m$ have been calculated.

Wind tunnel test rig design and experimental setup
Whilst having to consider the measurement of the necessary variables, the test rig would also need fit around the constraints of the wind tunnel. These considerations (in combination with the research in the literature review) eventually resulted in the final rig design seen below.

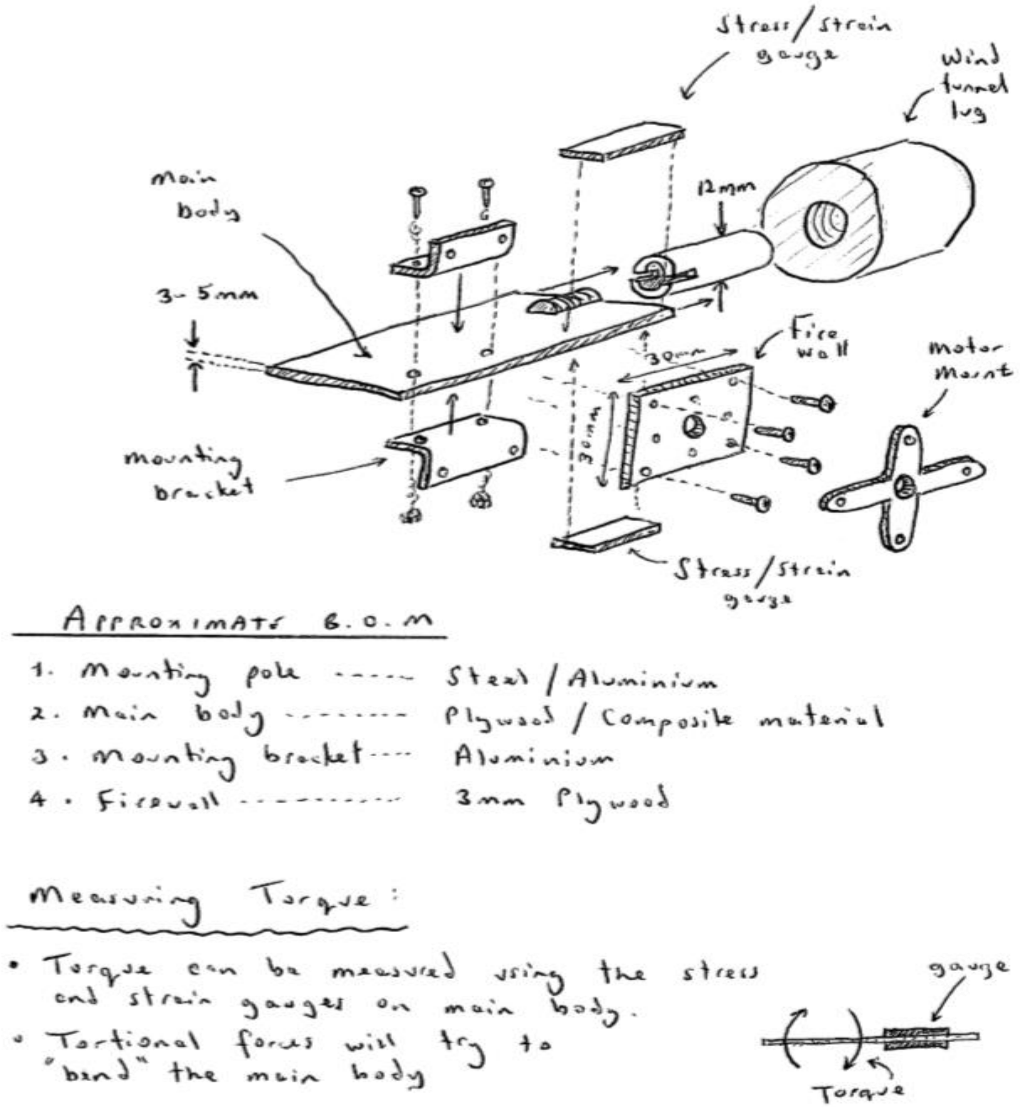


**Figure 20:** Wind tunnel test rig original design sketches

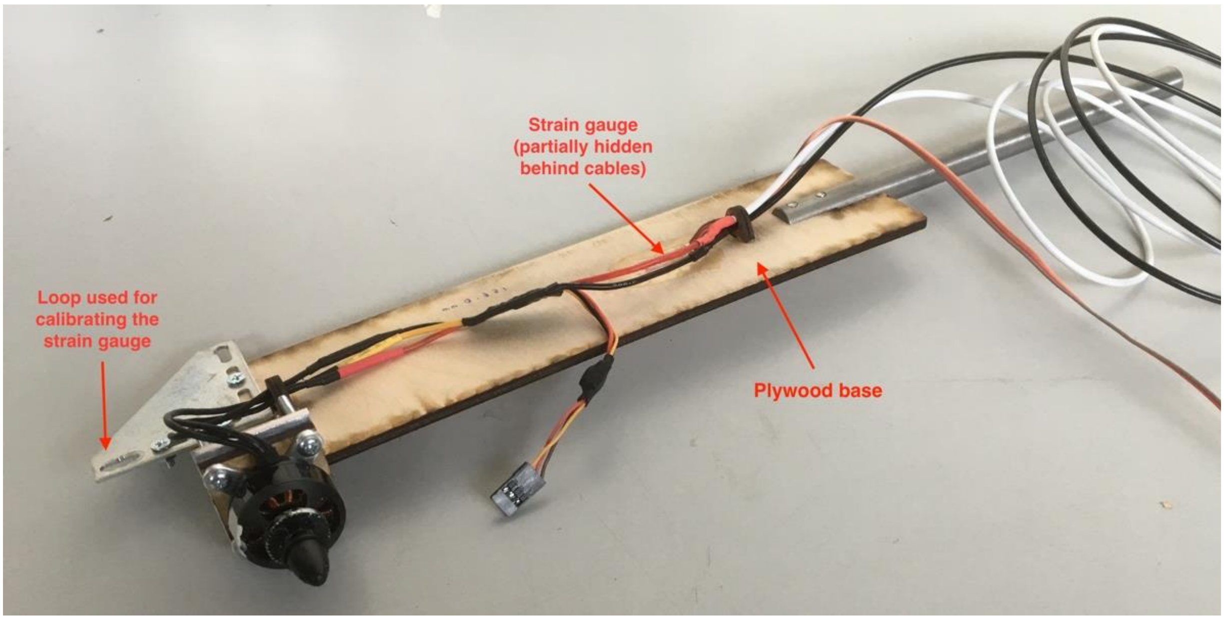


**Figure 21:** Wind tunnel test rig final revision

This rig was designed to fit the wind tunnel lugs so that the thrust produced by the propeller could be measured using the built-in instruments. $P_{in}$ was measured using the watt meter and *rpm* with the laser tachometer. The rig was also designed to measure torque through the use of a strain gauge attached to rigs upper surface. Most importantly, this would enable the actual $\eta_p$ and $\eta_m$ to be calculated through the use of Equation 2, Equation 3 and Equation 7 rearranged for $\eta_p$. The torque could, in theory, be measured by creating a linear relationship between torque and strain (calibrating the strain gauge with known loads – and thus bending moments - would allow this).

Regarding the setup of the experiments, the wind tunnels built-in load cells were calibrated through the application of known loads.

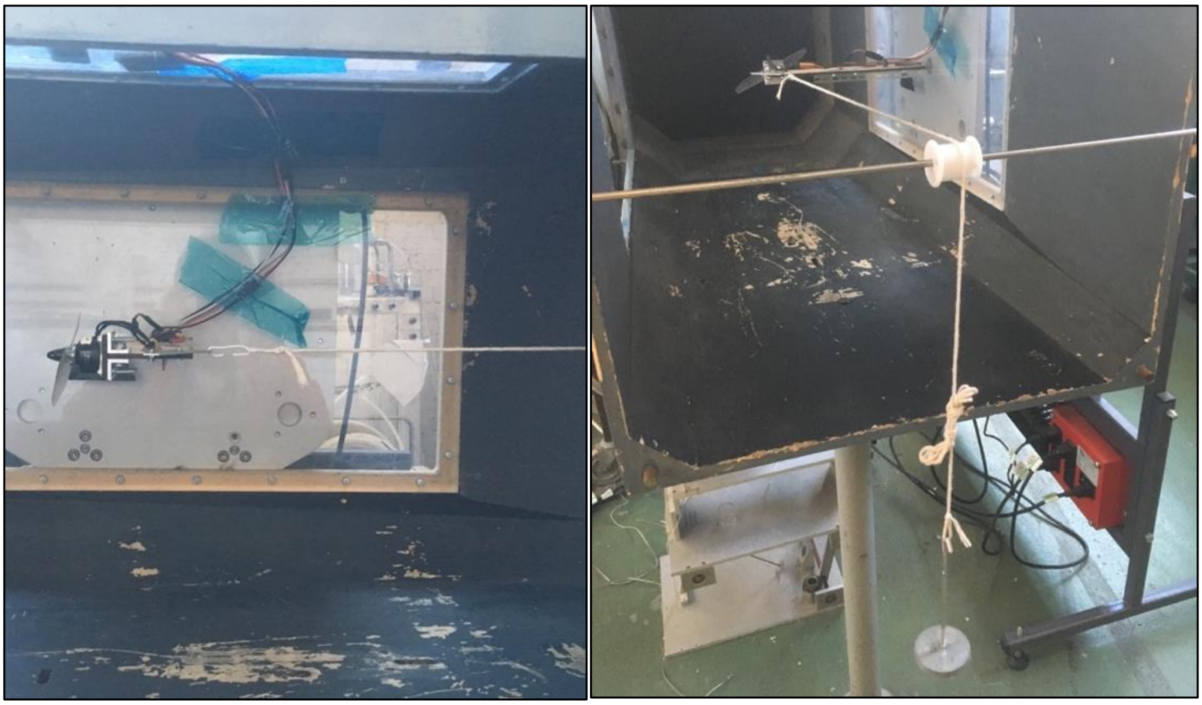

**Figure 22:** Wind tunnel load cell calibration

Additionally, the airspeed ($V_a$) was confirmed using both the built-in instruments as well as an external pitot tube set.

## Experiment methodology and execution

The experiments were performed using 2 separate approaches:

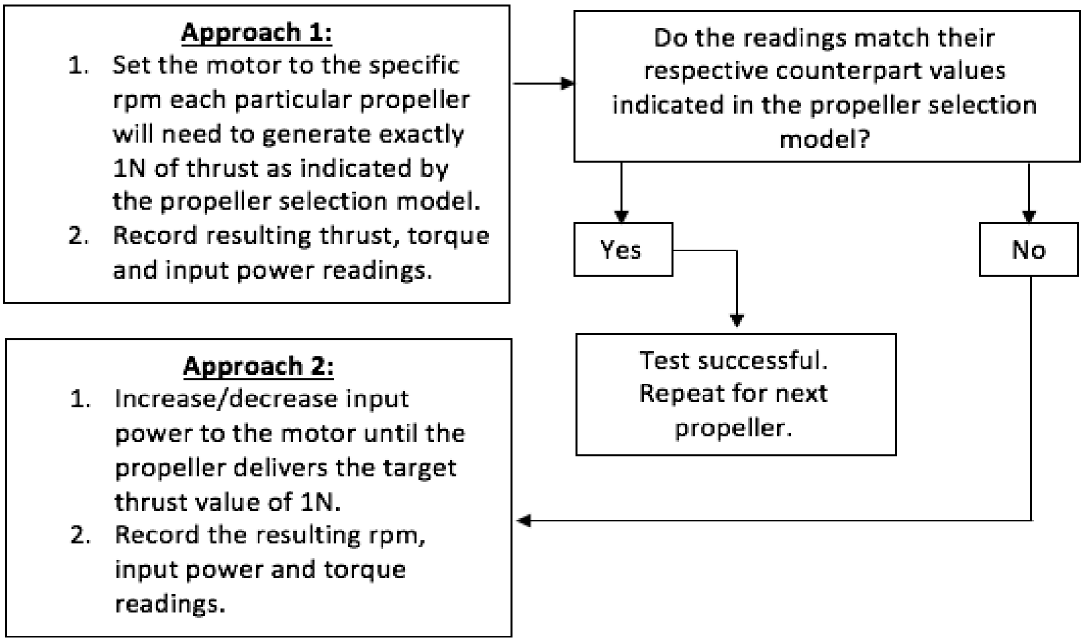


**Figure 23:** Wind tunnel testing procedures flow chart

Unfortunately, torque readings could ultimately not be recorded due to continuous issues with the strain gauge, which among other things included severe fluctuations in readings as a result of motor/propeller vibrations. The torque values could, however, still be calculated using a new regression based on the motor data obtained in previously from the experiments, using $P_{in}$ and *rpm* as the input variables.

In all, these tests were completed with 4 of the 8 propellers considered in the PSM, where the 7x5 propeller (deemed to be the most suitable by the PSM) was unfortunately unable to be tested due to complications with mounting it to the motor at the time.

## Results and observations

The following table of experimental results was produced:

**Table 3:** Wind tunnel test results

| WIND TUNNEL TEST DATA | | | | | | | |
|---|---|---|---|---|---|---|---|
| Target thrust = 1N Maximum achievable velocity = 13.5m/s | | | | | | | |
| APPROACH #1: Measured results based on target RPM | | | | | | | |
| **Prop** | Target RPM | Actual RPM | Thrust (N) | Input Power (W) | Torque (Nm) | Shaft Power | Propeller efficiency |
| **5x3** | 13150 | 13250 | 0.6 | 17.55 | 0.0040 | 5.53 | 1.47 |
| **5x4** | 10100 | 10080 | 0.2 | 12.4 | 0.0056 | 5.88 | 0.46 |
| **6x3** | 11250 | 11350 | 0.52 | 30 | 0.0159 | 18.70 | 0.38 |
| **7x3** | 11300 | 11380 | 0.5 | 15.6 | 0.0056 | 6.65 | 1.02 |
| APPROACH #2: Measured results based on exact target thrust | | | | | | | |
| **Prop** | Target thrust (N) | RPM | Input Power (W) | Torque (Nm) | Shaft Power | Propeller efficiency | |
| **5x3** | 1 | 15650 | 26.68 | 0.0073 | 12.04 | 1.12 | |
| **5x4** | 1 | 14500 | 39.60 | 0.0168 | 25.49 | 0.53 | |
| **6x3** | 1 | 15000 | 44.40 | 0.0188 | 29.57 | 0.46 | |
| **7x3** | 1 | 13350 | 28.08 | 0.0113 | 15.82 | 0.85 | |

As can be seen, not one of the propellers even gets close to producing 1N of thrust under the conditions indicated by the PSM. Note, however, that the supposedly “true” propeller efficiencies present here are clearly flawed, judging from their numerical values. Looking at the lower half of the table, each propeller required an additional few thousand *rpm*s before meeting the thrust requirement of 1N.

Accuracy, assumptions and limitations

The primary assumption here is that both physical and PSM propellers have identical geometry. Whilst they share the same rated properties, the rest could vary.

Additionally, the maximum achievable wind tunnel speed was 13.5 m/s as opposed to the target speed of 15 m/s (and its maximum rated speed of 16 m/s), likely due to the condition and cleanliness of the honeycomb section (Kyte, 2020). Moreover, this reduction in airspeed essentially overrides the effect of the wind tunnel airspeed corrections made using Glauerts methods (Equation 6), not only because the difference in airspeeds is larger than the calculated correction increments, but also because the corrections demand an airspeed slightly faster than the wind tunnels achievable maximum of 13.5 m/s.

The wind tunnel itself, being “open return” in design, may also have affected the accuracy of the readings. This design, whilst simple, can sometimes result in flow of relatively low quality across the test section (Hall, 2015).

Section conclusion

Although the differences between the PSM and physical propeller geometries may seem insignificant, they might well be responsible for the variations between their results. However, further validation is required before such conclusions can be made.

Whilst the difference in airspeeds would normally be of concern, it cannot be this that has caused the differences in thrust. After all, a lower airspeed should in essence increase the propeller’s $\alpha$, and thus its thrust, not reduce it. Therefore, even if an airspeed of 15 m/s was achieved, the conclusion effectively remains unchanged. Regarding the experimental propeller efficiencies, they are most likely unreliable due to the fact that they have been calculated using the new regression based on the inaccurate experimental motor data (see the “Experimental motor data” section above).

*JavaProp Analysis*

Aims of analysis

The aim here was to computationally analyse the performance of each propeller used in the wind tunnel experiments (and under the same operating conditions) to further determine the precision of the PSM.

Setting up the computational analysis

In order to analyse a propeller’s performance, JavaProp must first generate a virtual model of its blades. For this, it requires the chord length, the angle of attack, and the aerofoil type for each blade section provided. These were obtained using the process described below, roughly as advised by Mark Drela (Drela, 2005a).

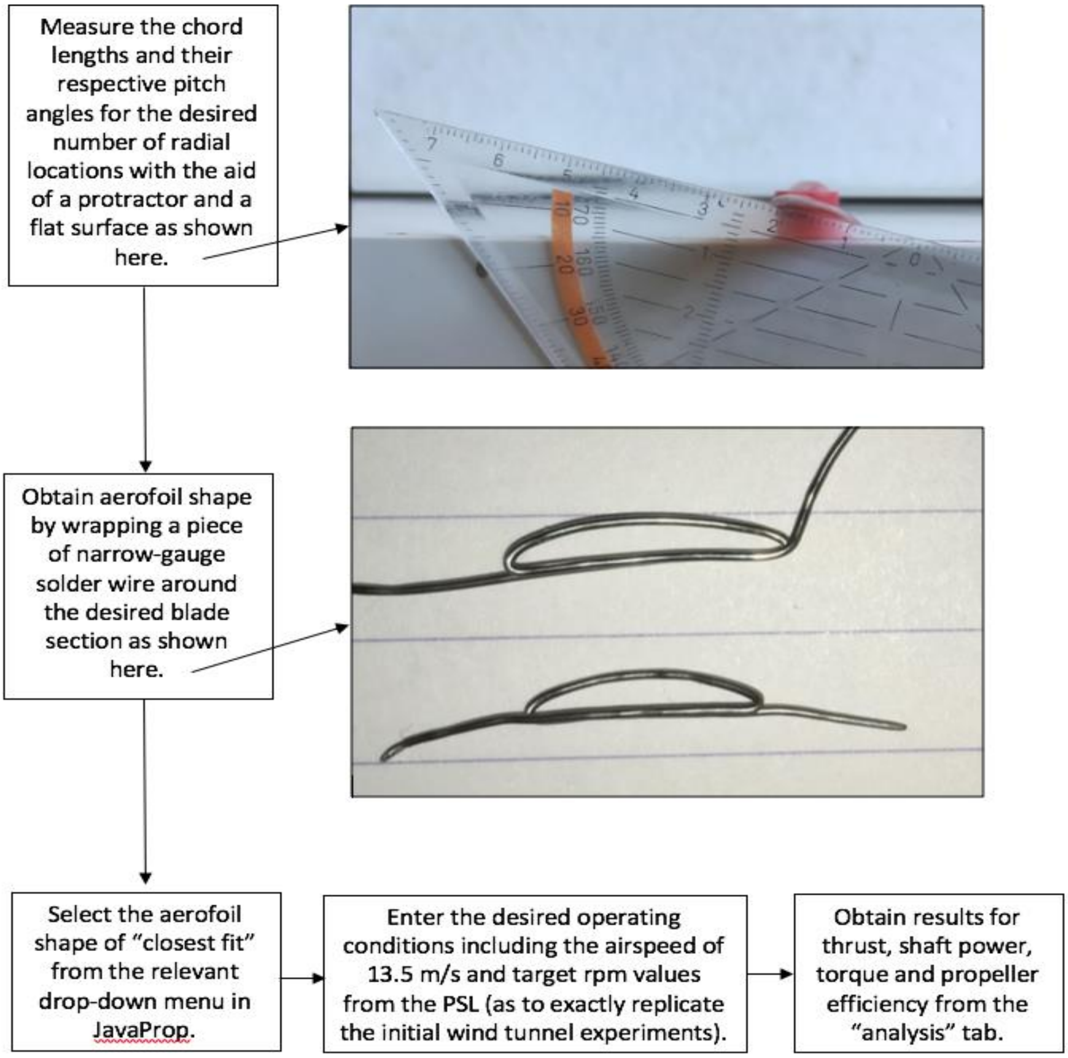


**Figure 24:** Flow chart for simulating propeller performance

## Results and observations

**Table 4:** JavaProp propeller analysis results

| JavaProp propeller analysis results | | | | |
|---|---|---|---|---|
| **Propeller type** | **Estimated thrust (N)** | **Shaft power (W)** | **Torque (Nm)** | **Peak efficiency (%)** |
| 5x3 | 0.55 | 14 | 0.011 | 52 |
| 5x4 | 0.25 | 5.5 | 0.0055 | 58 |
| 6x3 | 0.7 | 18.5 | 0.0155 | 57 |
| 7x3 | 0.6 | 11.5 | 0.0095 | 59 |

As seen in Table 4, the values for thrust match those from the experimental data in Table **3** reasonably well. Furthermore, when updating the $P_{in}$ values in Table **3** so that its $P_{shaft}$ values match those ones here, the values for torque are very similar as well, as seen in Table 5. This makes sense, as doing so effectively eliminates the use of the inaccurate regression based on the flawed experimental motor data. Hence, the $\eta_p$'s appear to be much more believable as well. The reason they don't match each other as closely as the torque values is likely due to the small variations in thrust (which directly influences $\eta_p$) between the two sets of results.

**Table 5:** Wind tunnel test results with updated shaft power values

| Measured results based on target RPM | | | | | | | |
|---|---|---|---|---|---|---|---|
| Prop | Target RPM | Actual RPM | Thrust (N) | Input Power (W) | Torque (Nm) | Shaft Power | Propeller efficiency |
| 5x3 | 13150 | 13250 | 0.6 | 26.2 | 0.0102 | 14.06 | 0.58 |
| 5x4 | 10100 | 10080 | 0.2 | 12 | 0.0052 | 5.53 | 0.49 |
| 6x3 | 11250 | 11350 | 0.52 | 29.7 | 0.0157 | 18.47 | 0.38 |
| 7x3 | 11300 | 11380 | 0.5 | 21 | 0.0097 | 11.46 | 0.59 |

<u>Accuracy and limitations</u>
One could consider the lack of 3D effects a limitation of JavaProp. Flow separation, for example, can substantially affect a propeller's drag, especially for high pitch propellers at relatively low airspeeds (Traub, 2016). However, this limitation likely carries little weight here, especially when compared to the differences in exact geometry of the physical and JavaProp propellers.

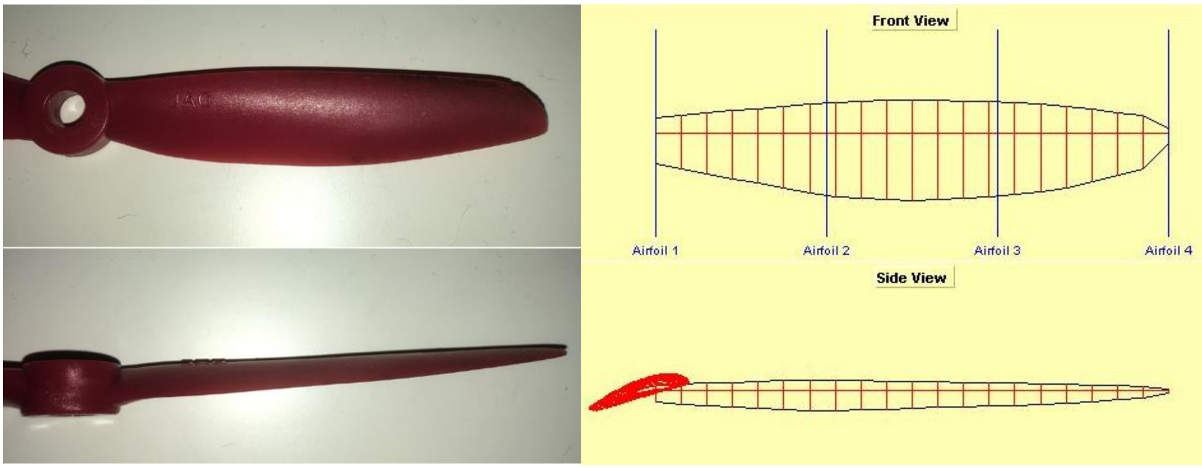


**Figure 25:** Physical vs computational propeller on JavaProp

The differences, although small, are due to the blade section measurements only being taken at several radial locations and also due to the lack of any inputs for other geometry features such as sweep, rake angles or exactly matching aerofoil shapes.

<u>Section conclusion</u>
Although the JavaProp and experimental results aren't identical (likely due to minor differences in exact blade shape), they clearly make those from the PSM stand out.

*Investigating the ideal propeller for the case study application*

<u>Aims</u>
Whilst not a true validation method as such, the idea of designing and building the ideal propeller was to ultimately create a benchmark from which to judge the most suitable off-the-shelf propeller established by the PSM. See the "Comparison between the 7x5 and theoretically ideal propellers" section below for the direct comparisons.

<u>Design and manufacture</u>

The ideal propeller's design was completed almost exclusively using JavaProp, and primarily revolved around maximising propeller diameter (considering the wind tunnel constraints) and thus efficiency potential, as stated in the literature review. The ideal propeller was, however, also designed around minimising the demand for *rpm* and shaft power. The design process of the ideal propeller has been outlined below:

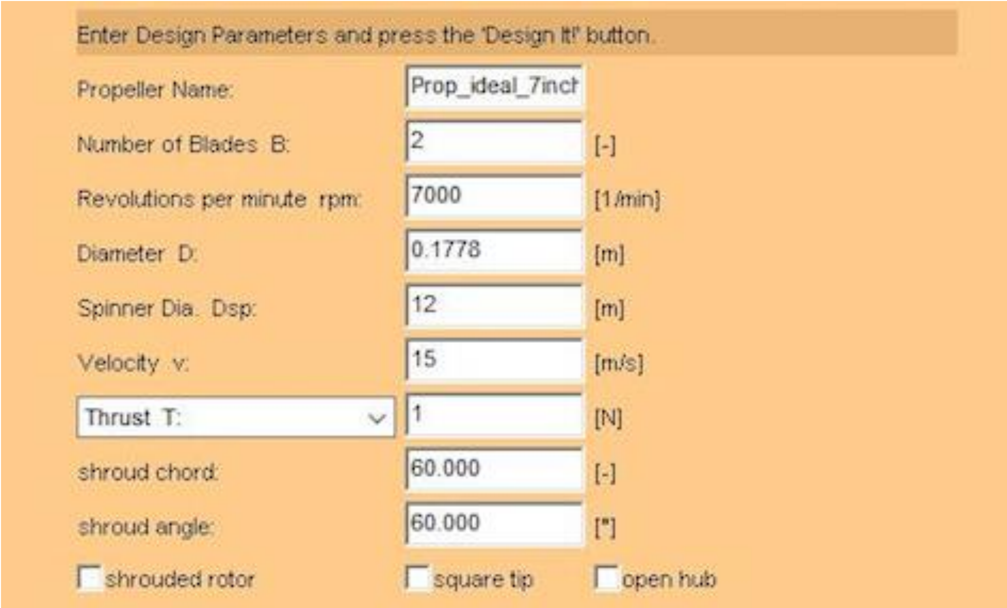


**Figure 26:** JavaProp input menu

Figure 26 represents the propeller design input menu of JavaProp. As stated, maximising a propellers diameter whilst minimising its pitch maximises its efficiency. Consequently, a diameter of 7 inches (0.1778 m) was chosen (as to still satisfy the wind tunnel constraints).

Having specified the desired airspeed of 15 m/s, the next design step attempted to minimise the demand for shaft power and thus the power consumption of the motor. This was achieved by adjusting the desired *rpm* until the indicated shaft power requirement would go no lower. Note: had the experimental motor operating data have produced a more reliable 3D regression (described previously), then this propeller would have been designed around the motors most efficient operating point, and not by minimising the *rpm* and shaft power requirements.

The next step included defining the aerofoil types at 4 separate radial stations. The followings ones were selected according to suggestions within the JavaProp user manual.

**Table 6:** Aerofoil distribution along length of blade

| Radial position r/R | Aerofoil type selected | Reason for selection | Representation of shape |
|---|---|---|---|
| 0 | MH126 | Offeres a strong root section |  |
| 0.33 | MH112 | Often used for section following the root |  |
| 0.67 | Clark Y | Well suited for sections beyond 50% blade length |  |
| 1 | MH116 | Most efficient for blade tips operating below Mach 0.6 |  |

As it turns out, these were suitable choices, as subsequent calculations proved that the blades minimum cross-sectional area was just about sufficient for enduring the intended load.

Having completed this, the propeller could finally be generated. Since JavaProp functions according to the principles of “the optimum propeller” with minimum induced loss, that means it will always design the most efficient propeller around the given parameters. This ideal propeller took the following form:

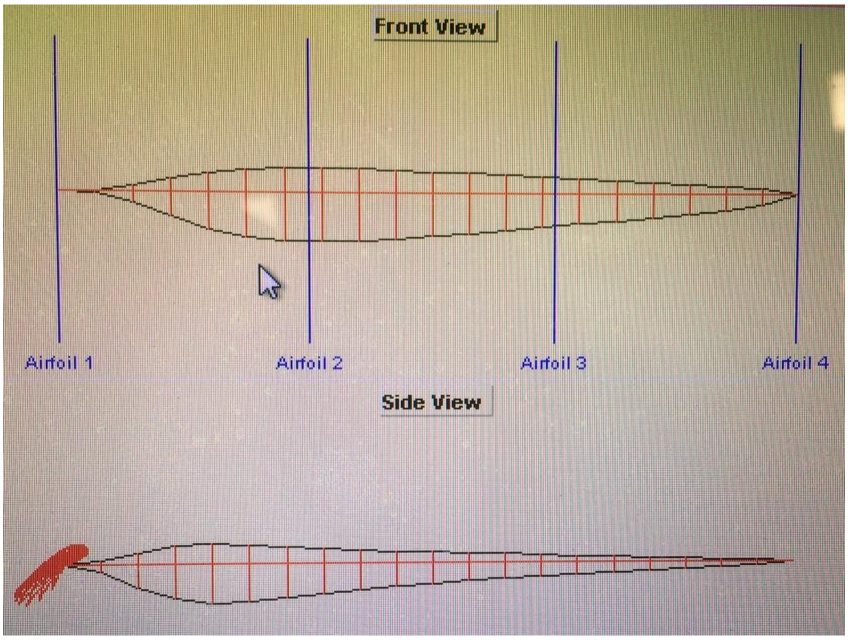


**Figure 27:** Ideal propeller blade geometry as previewed in JavaProp

This blade geometry was exported to Solidworks and subsequently modelled into a complete propeller including a hub. Various regions, including the trailing edge and propeller tips additionally needed to be thickened slightly to satisfy the 3D printers minimum thickness requirement before the manufacture process could take place.

Note: Since this “blade thickening” would effectively increase the propeller’s drag and lower efficiency, a second, modified version of one the off-the-shelf propellers featuring thickened features was also produced to give the ideal propeller a fair comparison. The 5x4 propeller was chosen here for its relatively simple geometry and ease of design.

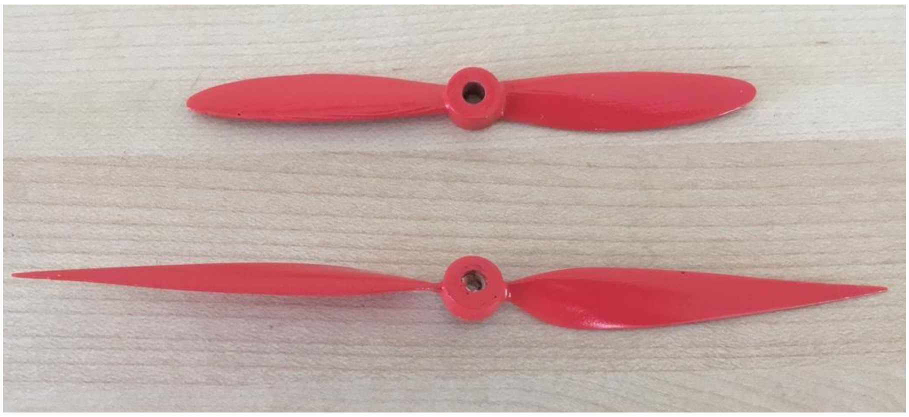

**Figure 28:** Completed ABS ideal (bottom) and modified 5x4 (top) propellers

Figure 28 above presents the completed propellers, each one having been sanded and given a coat of spray paint in an attempt to enhance their surface finish.

Performance predictions of ideal propeller

Figure 29, among other things, presents the propeller's expected efficiency of 80.9% at a shaft power of approximately 15.75W (Figure 30) under the given operating conditions as calculated by JavaProp.

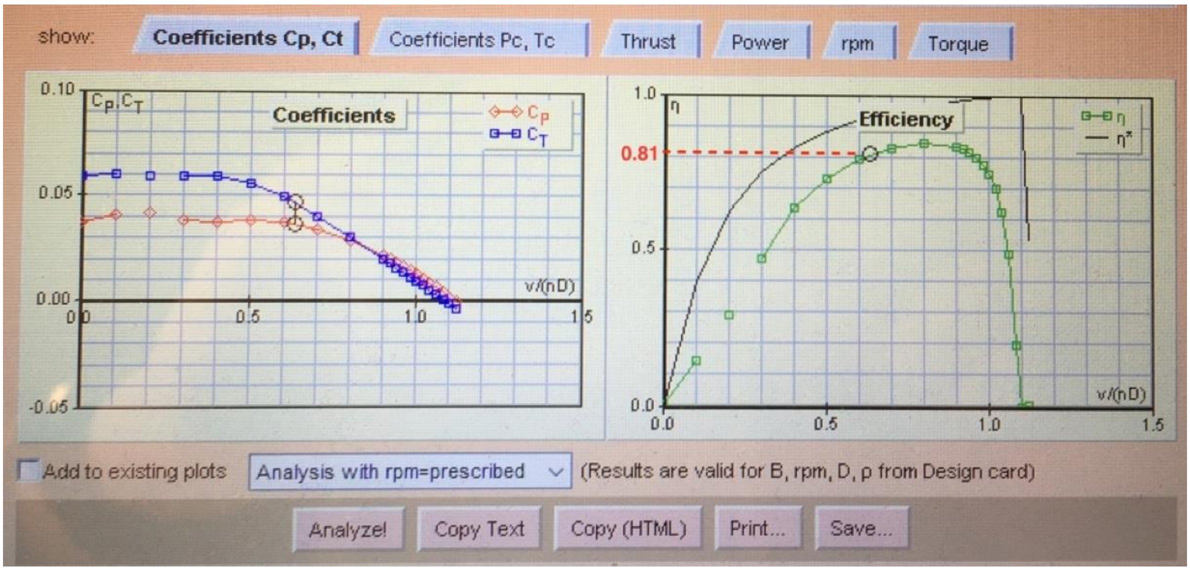


**Figure 29:** Ideal propeller efficiency plot

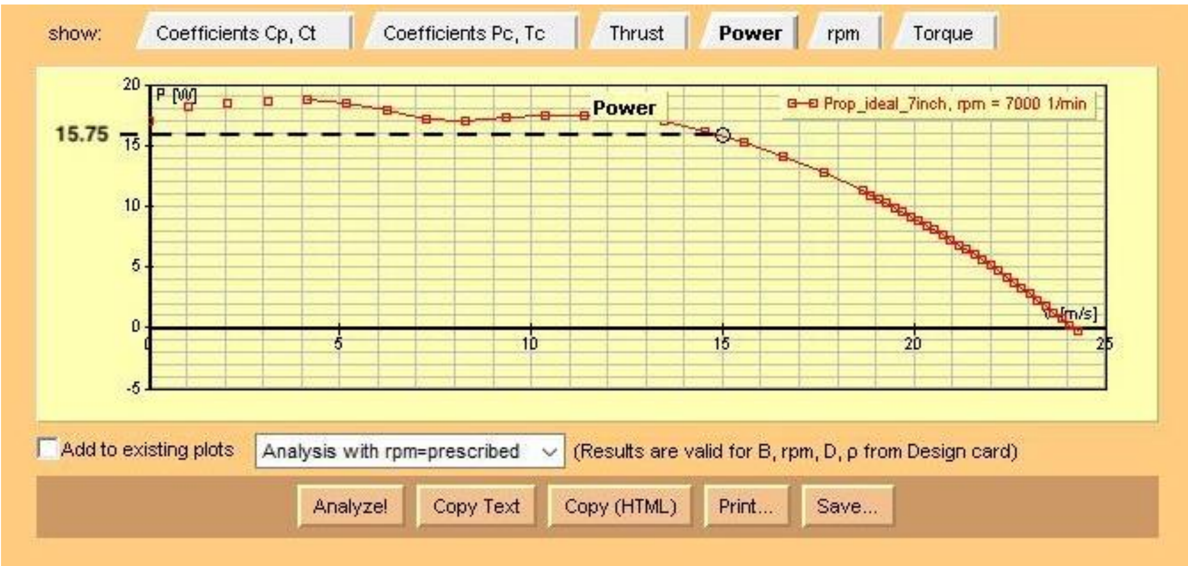


**Figure 30:** Ideal propeller shaft power plot

Experiments and testing

Testing these physical propellers would indicate the accuracy of JavaProp's ideal propeller design, and thus its efficiency predictions. Unfortunately, experiments could not be completed using the wind tunnel before the universities early closure in March 2020 as a result of the Coronavirus pandemic. As such, only static tests could be completed at home using a simple Meccano rig and kitchen scales. Thrust from the propeller was translated to the scales via an 'L' shaped lever with two arms of equal length.

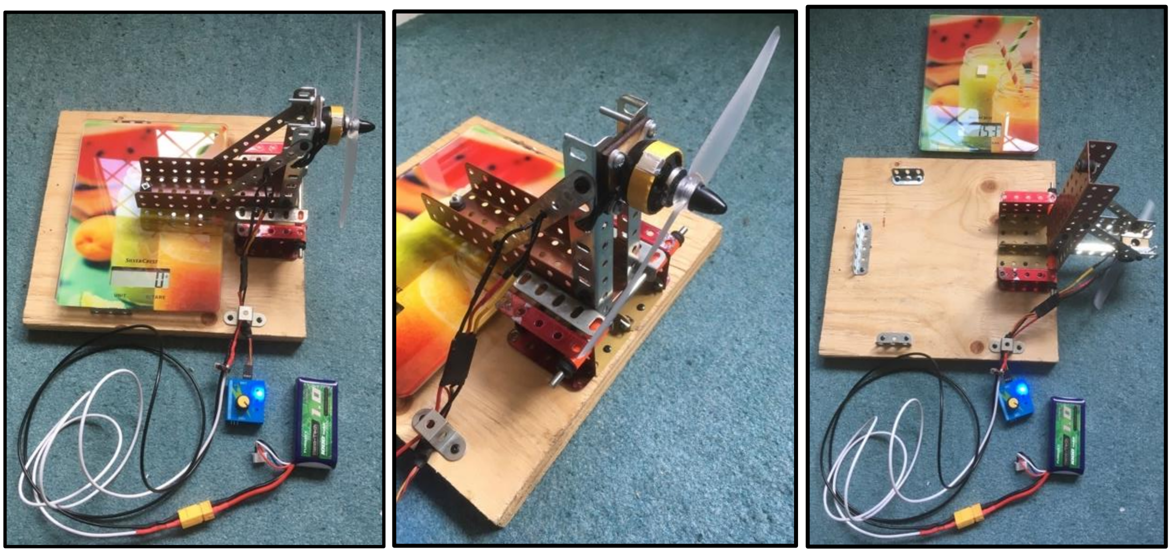

**Figure 31:** Meccano static test rig

Thrust was initially measured in grams whilst the motor speed was measured in Hz using the audio based mobile application "Sonic Tools". As before, input power was measured using the watt meter. The experimental procedure was simply to measure the frequency and input power at which 1N (or 102g) of thrust was produced, and to compare these to the static JavaProp predictions for each propeller. Whilst the real-life propeller efficiencies couldn't be obtained under the given circumstances (they would be zero under static conditions anyway), these experiments could still assist in judging JavaProps design accuracy and thus the $\eta_p$ prediction of 80.9%. The original 5x4 propeller (from which the modified version was modelled) was also tested to see how the accuracy of these static tests compared to those of the wind tunnel.

Results and observations

Table 7 presents the experimental results, where the thrust readings were multiplied by 9.81/1000 to give their values in Newtons.

**Table 7:** Static propeller experimental results

| Static propeller experimental results | | | | | |
|---|---|---|---|---|---|
| Propeller | Speed (Hz) | Speed (RPM) | Thurst (g) | Thrust (N) | Input power (W) |
| Ideal 7 inch | 321 | 9630 | 102 | 1.00 | 77.88 |
| 5x4 "fat" | 497 | 14910 | 103 | 1.01 | 30.68 |
| Original 5x4 | 440 | 13200 | 103 | 1.01 | 33.88 |

The motors speed was converted from Hz to *rpm* using the following equation:

$$Since: \quad Hz = \frac{RPM \times Number\ of\ blades}{60} \quad \text{(Buckingham et al., 2002)}$$

$$Therefore \ldots \quad rpm = \frac{Hz \times 60}{Number\ of\ blades}$$

**Equation 8**: Hz to rpm

Figure 32 below presents the JavaProp static thrust predictions (red arrows) for each propeller at the *rpm*s measured during the tests.

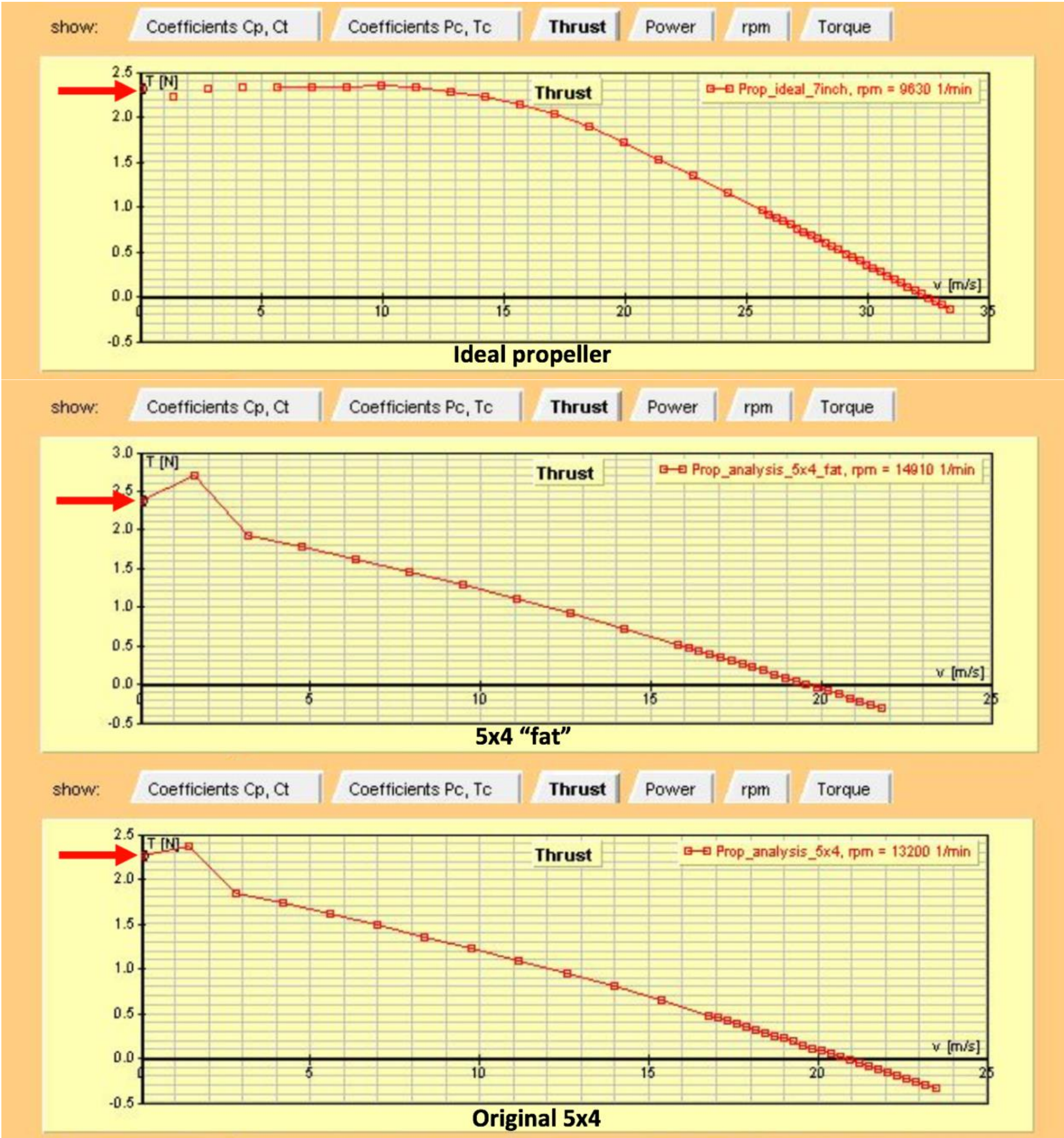


**Figure 32:** JavaProp static thrust predictions

**Table 8:** Static test vs JavaProp thrust comparison

| Static rig vs JavaProp Thrust (N) | | |
|---|---|---|
| **Propeller** | **Static rig** | **JavaProp** |
| Ideal 7 inch | 1.00 | 2.32 |
| 5x4 "fat" | 1.01 | 2.36 |
| Original 5x4 | 1.01 | 2.26 |

As can be seen in Table 8, the experimental results appear to be out by a factor of around two for each of the propellers.

Accuracy and limitations

As can be expected, the apparatus used to conduct the static experiments leaves a lot to be desired, limiting their accuracy considerably. First and foremost, the precision of the audio-based frequency meter used for measuring the motor speed is likely low, despite its readings first being validated against those taken on other audio-based applications with positive results.

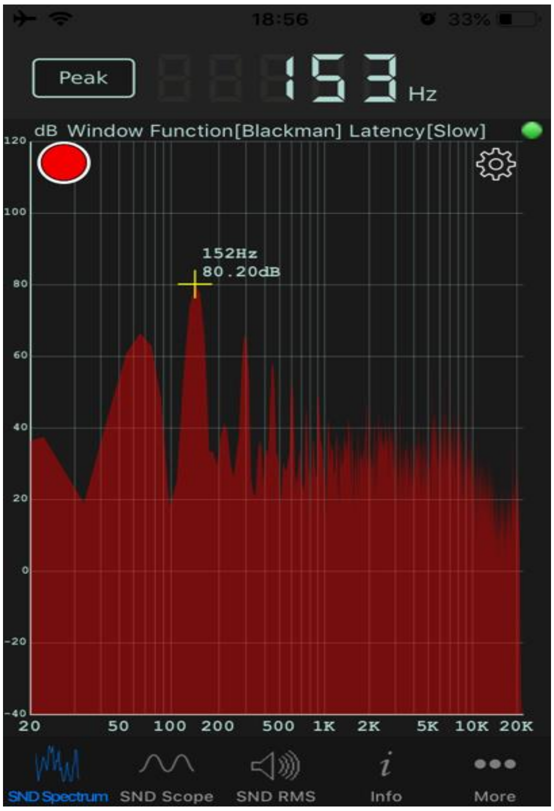


**Figure 33:** Sonic Tools measurement window snippet

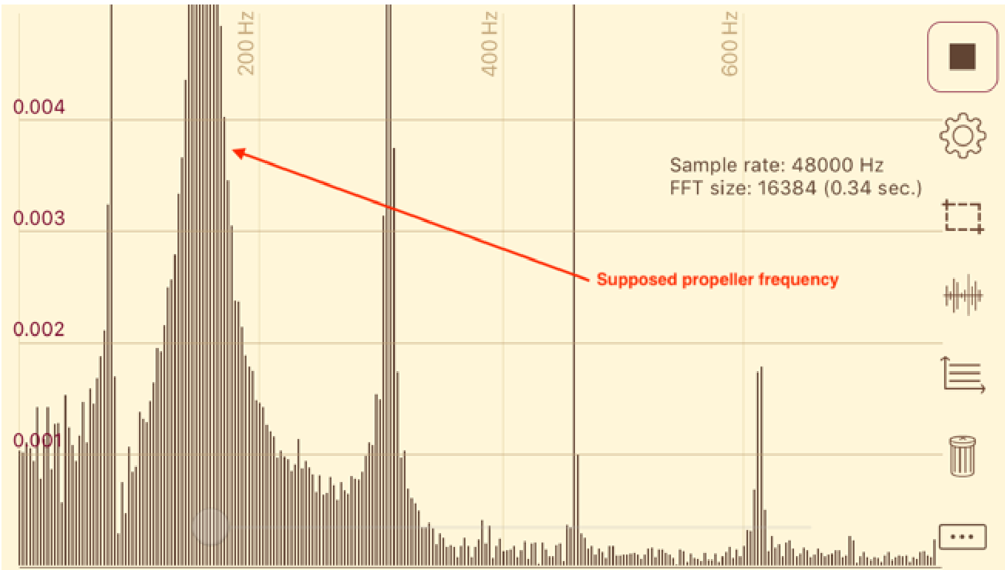


**Figure 34:** "Soundspectrum" measurement window snippet

Figure 34 above shows and example of readings taken on the alternative frequency meter application “Soundspectrum”, and it clearly indicates a fair amount of background noise which might be distorting the readings of both applications.

It is also possible that the physical propeller geometry (not to mention the modifications made in SolidWorks) have had an effect on the results. For example, the surface finish of the 3D printed propellers, whilst improved by sanding and spray paint, is still far from perfect. Depending on severity, this will increase the blades Reynolds numbers and drag especially at the blade tips, which can increase the drag of each blade by around 10% (Krüger, Kornev & Greitsch, 2016). The exact effects of surface roughness in this case are, however, difficult to determine, especially with the lack of lab equipment and resources.

Lastly, the rig itself might actually be disrupting the airflow in front of the propeller which might be contributing to the inaccuracies present.

<u>Section conclusion</u>
Whilst the results seem inconclusive, the fact that they are all consistently out by the roughly same factor when compared to JavaProp is of significance. Furthermore, the results from the original 5x4 are also out by a similar factor, where JavaProp seemed to replicate the wind tunnel results for this very same propeller quite well. Due to this, (and the lack of any other validation) it is safe to conclude that these experiments were inaccurate primarily due to the apparatus used, and it can thus be said with some confidence that the JavaProp design outputs are of acceptable accuracy.

## Comparison of results and final explanations

### Comparison between the PSM and validation results

*Data comparison charts*
Figure 35 and Figure 36 present charts of the propeller thrust and efficiency values from the PSM and each of respective validation methods.

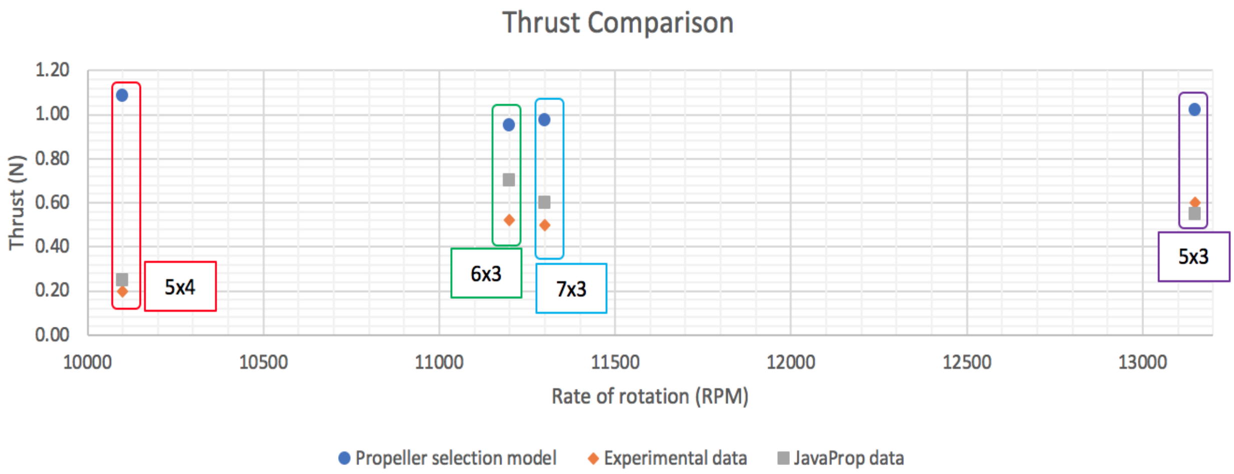


**Figure 35:** Propeller thrust comparison

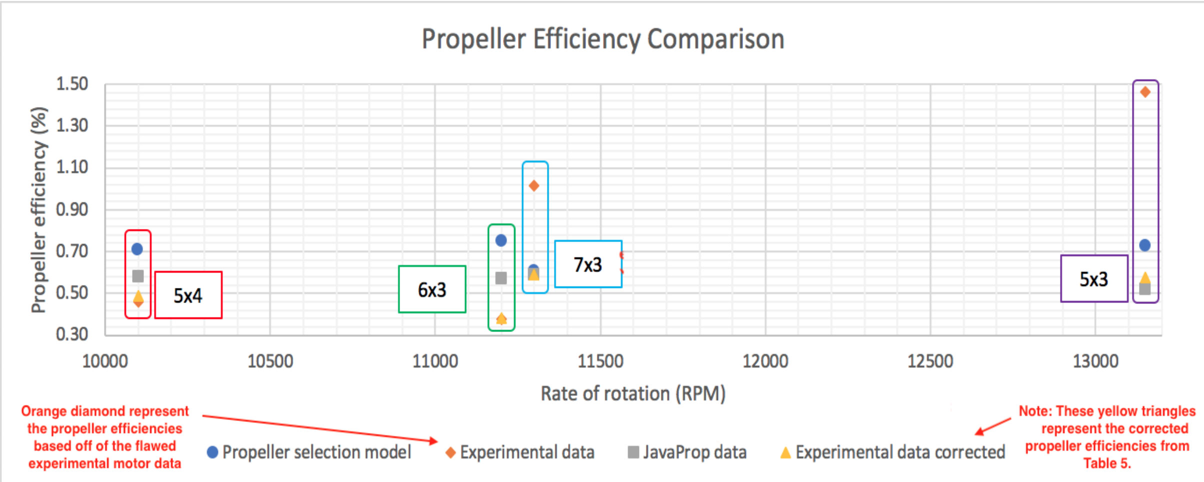


**Figure 36:** Propeller efficiency comparison

As can be seen, whilst there is disparity between all the results, the PSM results stand out the most predominantly, especially with respect to thrust. Note; had the PSM results been based off of an airspeed of 13.5 m/s as well, then their thrust values would be greater still.

*Final explanations for the variation in the results*

Regarding the smaller differences between the 2 validation methods results for both thrust and efficiency, these are, to reiterate, likely due to the slight variations in exact blade shape present in JavaProp.

However, the differences between the PSM and physical propeller geometry, are probably, as previously stated, much greater. Especially crucial towards the tip (the region of greatest thrust/efficiency influence), differences in blade shape become increasingly significant with higher *rpm*, where larger blade areas increase thrust output. Studies show that different propellers with identical rated properties can still experience thrust percentage differences of 34.3% regardless (Master Airscrew, 2016), with slightly differing chord distributions alone have a notable influence on propeller performance, including a 3% difference in efficiency (Toman et al., 2019).

The image below illustrates how much tip geometry alone can vary between propellers.

***Figure 37:*** *Varying propeller geometry – especially the tips*

Furthermore, whilst the physical propellers were generally all very cheap components, the ones embodied in the PSM are high quality and "competition proven" (apcprop.com, 2019), further justifying their apparently superior performance.

Lastly it is also possible that the raw data in the PSM is itself somewhat flawed, as the NASA Analysis Program from which it originates tends to "underpredict propeller drag at lower (air)speeds" (apcprop.com, 2019). Unfortunately, exactly what the program considers "lower speed" (and thus the impact on the data's "low speed" accuracy) remains unknown.

## Comparison between the 7x5 and theoretically ideal propellers

**Table 9:** Comparison between ideal and best off-the-shelf propellers

| Ideal propeller and 7x5 comparison | | | | |
|---|---|---|---|---|
| **Propeller** | **RPM** | **Shaft Power (W)** | **Propeller efficiency (%)** | **Motor efficiency (%)** |
| Ideal | 7000 | 15.75 | 80.89 | 0.523443507 |
| 7x5 | 7250 | 19 | 84.36 | 0.521324799 |

Through comparison of the theoretical data alone, both of these propellers seem quite evenly matched. However, the 7x5 actually appears to have a slightly greater individual efficiency (based on the $\eta_p$ regression) than the so-called ideal propeller. This is likely because the ideal propeller, unlike the 7x5, has been designed around the entire propulsion system, and therefore aims to minimise *rpm* and $P_{shaft}$ to improve $\eta_m$ and power consumption. Although the calculated motor efficiencies have been included above for completeness, please note that these have once more been obtained using the flawed $\eta_m$ regression and should be approached with scepticism.

However, it is important to remember that the ideal propeller has been "thickened" for the feasibility of 3D printing. By comparing the efficiency of the modified 5x4 to that of the original 5x4 under 1N of thrust in JavaProp, it is quite clear to see that the original is about 2% more efficient, as indicated in Figure 38 and Figure 39.

Although the variation in efficiency values cannot be applied directly to the ideal propeller, it does indicate that it would most likely perform better if not constrained by the manufacturing restrictions and would have a similar or perhaps even better efficiency than the 7x5.

Note: a direct JavaProp analysis of the 7x5 was not been included here, as the physical propeller from which the virtual model would be based off likely has different "non-rated" geometry to the 7x5 used in the PSM.

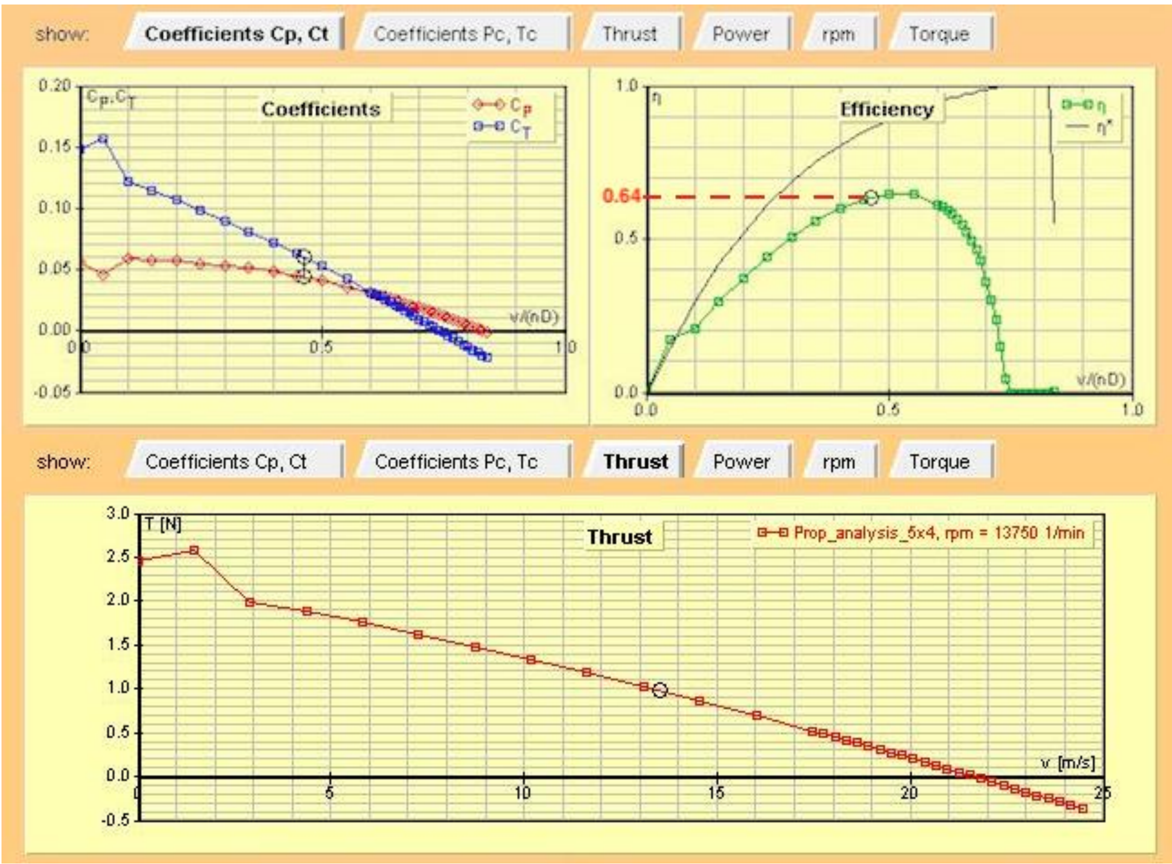


**Figure 38:** JavaProp original 5x4 propeller performance at 1N of thrust

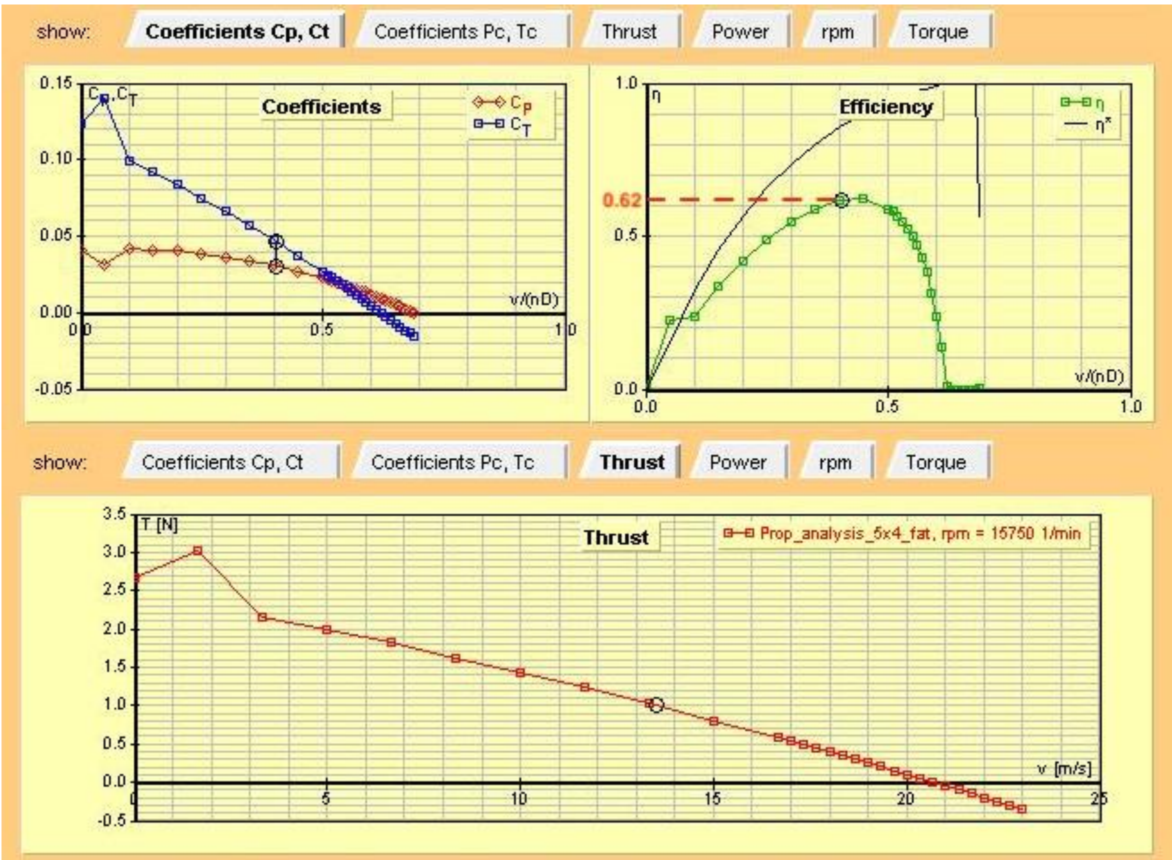


**Figure 39:** JavaProp modified 5x4 propeller performance at 1N of thrust

**Secondary case study requirements - achieving take-off thrust**
Fortunately, due to solving the previous complications with attaching the 7x5 propeller to the motor, it too could be tested under static conditions solely for the purpose of proving that it could provide the 3.9N of take-off thrust stated among the "Case study operating parameters". Note, however, that without the use of the wind tunnel, it could not be proven that this thrust could be provided under dynamic conditions.

**Table 10:** 7x5 static take-off thrust experimental results

| Static 7x5 experimental results | | | | | |
|---|---|---|---|---|---|
| Propeller | Speed (Hz) | Speed (RPM) | Thurst (g) | Thrust (N) | Input power (W) |
| 7x5 | 309 | 9270 | 399 | 3.91 | 320 |

As seen in Table 10, the thrust requirement of 3.9N was indeed met at the indicated r*pm* and input power. Note that the ideal propeller failed to meet these requirements. Looking back at the literature review, this is likely because it was designed with the sole purpose of generating just 1N of thrust at maximum efficiency, and thus does not perform well outside of its intended operating conditions.

## Final conclusions

To conclude, the differences in results between the PSM and the validation methods are most probably the product of:

- the propellers likely having varying blade geometry, despite the same "rated" properties.
- the physical propellers being cheap components of considerably lower quality than the ones embodied in the PSM.
- the possibility that the PSM data itself is slightly flawed as a result of the NASA Analysis Program underpredicting propeller drag at "lower airspeeds".

This aside, the only apparent issue with the PSM itself is the questionable accuracy of its regressions, the $\eta_m$ regression in particular. As established, this was down to the quality of the experimental setup used to obtain the motor data, and it is now clear that such experiments need to be completed using high precision apparatus in order to produce feasible results.

However, the PSM has proven itself to be a functional tool, limited only by the quality of its input data and regressions. Such a tool, in the hands of a model aircraft propeller manufacturer with the means to obtain accurate experimental data for both the propellers and motor, could well improve its accuracy potential and practicality.

Regarding the requirements of the case study, the "Comparison between the 7x5 and theoretically ideal propellers" conclusion above indicates that the PSM's selected 7x5 propeller is indeed a good choice, due to it meeting both cruise and take-off thrust requirements, and due to its apparent similarities with the (admittedly poorly validated) ideal propeller.

## Recommendations

These recommendations include things which might improve the PSM in its current form, but also things that could have improved the practical elements of this investigation.

### Propeller selection model recommendations

As the propeller data obtained from apcprop.com does not specify anything other than the propeller's rated geometry, modelling the PSM off of experimental data obtained from physical propellers with precisely known geometries would greatly improve its practicality. Additionally, equipping the PSM with some sort of function for choosing the relevant propeller type (e.g. bullnose, raisbeck or even a particular manufacturer) would further enhance its durability. It goes without saying that the PSM's scope would ideally need to be broadened by including the data from as many different propellers as possible, and not just the ones relevant to the case study.

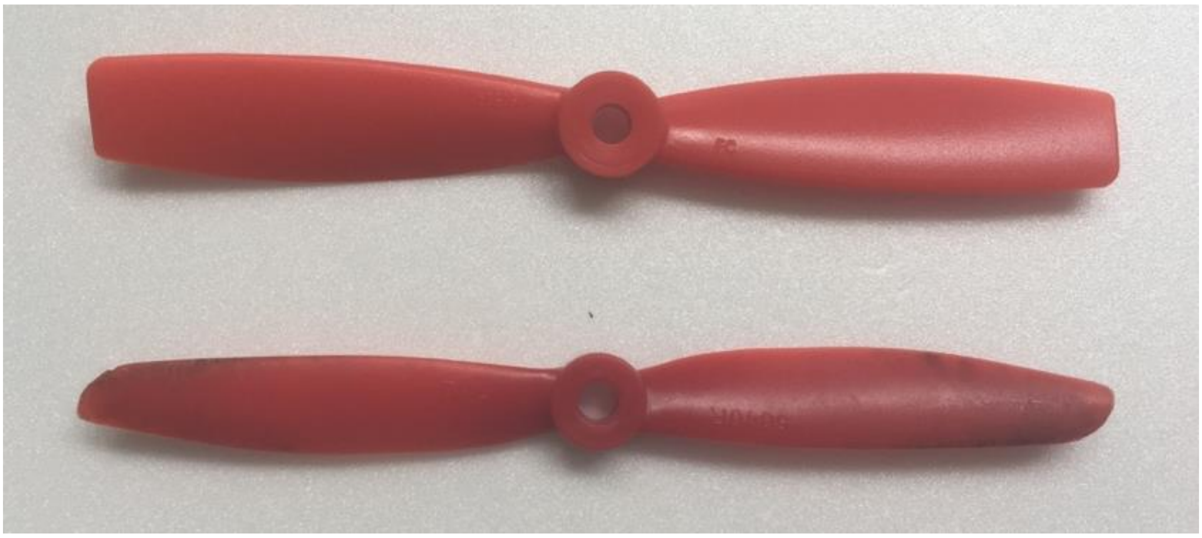

**Figure 40:** Bullnose propeller vs standard propeller

### Practical elements recommendations

The rig used to obtain the regression for $\eta_m$ should, as previously mentioned, have featured supports either side of the motor mount with actual ball bearings to reduce its rotatory friction and thus improve the rig's accuracy.

Furthermore, had the wind tunnel test rig have been made from a much stiffer material than plywood, this would at least partially have solved the issues with the strain gauge and would thus have provided perhaps useable readings for torque. Alternatively, the torque could perhaps have been measured through the use of a load cell once more. Regrettably, experimentation with such methods was not possible due to the universities unexpected closure.

Regarding the ideal propeller design, it should have featured an extra validation mode to ensure that JavaProps predictions were correct. Whilst the propeller design methods of Mark Drela were investigated in some detail, time and resources for its implementation unfortunately ran out.

**Acknowledgements**

I would like to thank Adam Kyte for his continuous guidance throughout the formulation of this paper and for addressing my many questions. I would also like to thank Chris Pass for his support in Adam Kyte's absence, and the numerous lab staff for assisting the practical elements of this investigation. These include Richard Cullen, Jeremy Clark, Hannah Poulson, Alastair Reynolds, Andrew Oxenham, and Neil Fewings.

## List of abbreviations

| Abbreviation | Definition |
|---|---|
| ESC | Electronic speed controller |
| PSM | Propeller selection model (used extensively) |

## Nomenclature

| Symbol | Definition | Units |
|---|---|---|
| $B$ | Number of propeller blades | - |
| $C_D$ | Airframe drag coefficient | - |
| $D$ | Propeller diameter | m or inches |
| $F_D$ | Airframe drag force | N |
| $J$ | Advance Ratio | - |
| $L_C$ | Rated propeller chord length | m |
| $P_{in}$ | Input power | W |
| $P_{shaft}$ | Motor shaft power | W |
| $Q$ | Torque | Nm |
| $R^2$ | Coefficient of determination | - |
| $Re_{Lc}$ | Rated chord length-based Reynolds number | - |
| $S$ | Flying wing total surface area | $m^2$ |
| $T$ | Propeller thrust | N |
| $V_a$ | Forward airspeed | m/s |
| $W$ | Relative airflow velocity across blade element | m/s |
| $kv$ | Motor velocity constant | Revolutions/volt |
| $n$ | Motor/propeller revolutions per second | 1/s |
| $rpm$ | Motor/propeller revolutions per minute | 1/min |
| $\alpha$ | Angle of attack | ° |
| $\beta$ | True geometric pitch | ° |
| $\gamma$ | Climb angle | ° |
| $\eta_m$ | Motor efficiency (includes ESC efficiency) | - |
| $\eta_p$ | Propeller efficiency | - |
| $\rho$ | Air density | $kg/m^3$ |
| $\varphi$ | Relative flow angle | ° |
| $\omega r$ | Perpendicular velocity component | m/s |

## References

**Aberle, B.** (2016) 'How Do I Learn the Basics of Electrical Power for Models?'. [Online]. Available at: http://amaflightschool.org/getstarted/how-do-i-learn-basics-electrical-power-models (Accessed: 09/04/2020).

**apcprop.com.** (2019) 'APC Propellers'. Quality Propellers that are Competition Proven. [Online]. Available at: https://www.apcprop.com.

**Avanzini, G., de Angelis, E. L. & Giulietti, F.** (2016) 'Optimal performance and sizing of a battery-powered aircraft'. Aerospace Science and Technology, 59 pp. 132-144.

**Barlow, J. B., Rae, W. H. & Pope, A.** (1999) 'Low-speed wind tunnel testing'.

**Bass, R.** (1986) 'Small scale wind tunnel testing of model propellers', 24th Aerospace Sciences Meeting. pp. 392.

**Brandt, J. & Selig, M.** (2011) 'Propeller performance data at low reynolds numbers', 49th AIAA Aerospace Sciences Meeting including the New Horizons Forum and Aerospace Exposition. pp. 1255.

**Buckingham, M. J., Giddens, E. M., Simonet, F. & Hahn, T. R.** (2002) 'Propeller noise from a light aircraft for low-frequency measurements of the speed of sound in a marine sediment'. Journal of Computational Acoustics, 10 (04), pp. 445-464.

**Drela, M.** (2005a) 'Propeller Characterization for QPROP'. URL: http://web.mit. edu/drela/Public/web/qprop/prop_measure.pdf

**Drela, M.** (2005b) 'DC Motor/Propeller Matching'. Lecture Notes, 1 (5), pp. 1-6.

**Eppler, R. & Hepperle, M.** (1984) 'A procedure for propeller design by inverse methods', International Conference of Inverse Design Concepts in Engineering Sciences. pp. 445-460.

**Fitzgerald, R. E.** (2007) Wind tunnel blockage corrections for propellers.

**Gabriel, D. L., Meyer, J. & Du Plessis, F.** (2011) 'Brushless DC motor characterisation and selection for a fixed wing UAV', IEEE Africon'11. IEEE, pp. 1-6.

**Garner, W.** (2009) 'Model airplane propellers'. Air-Propeller research document, wbgarner08@ verizon.net

**Gerr, D.** (2001) Propeller handbook : the complete reference for choosing, installing and understanding boat propellers. New York ; London: New York ; London : McGraw-Hill.

**Gur, O. & Rosen, A.** (2005) 'Propeller performance at low advance ratio'. Journal of aircraft, 42 (2), pp. 435-441.

**Hall, N.** (2015) 'Open return wind tunnel'. Wind tunnels, National Aeronautics and Space Administration. [Online]. Available at: https://www.grc.nasa.gov/WWW/K-12/airplane/tunoret.html (Accessed: 13/03/2020).

**Hepperle, M.** (2010) 'JavaProp Users Guide'.

**Hitchens, F.** (2015) Propeller aerodynamics: the history, aerodynamics & operation of aircraft propellers. Andrews UK Limited.

**Kane, J.** (2020) 'Basic Information to Help Select the Correct Propeller'. Propeller Performance Factors [Online]. Available at: http://www.epi-eng.com/propeller_technology/selecting_a_propeller.htm (Accessed: 11/11/2019).

**Krüger, C., Kornev, N. & Greitsch, L.** (2016) 'Influence of propeller tip roughness on tip vortex strength and propeller performance'. Ship Technology Research, 63 (2), pp. 110-120.

**Kyte, A.** (2019) 'Foil Theory and Wind Tunnel Testing'.

**Kyte, A.** (2020) 'Verbal'.

**Martinez, I.** (2009) 'Propellers'. Propulsion, Ciudad Universitaria. [Online]. Available at: http://webserver.dmt.upm.es/~isidoro/bk3/c17/Propellers.pdf (Accessed: 14/10/2019).

**Master Airscrew.** (2016) 'Master Airscrew vs APC Propeller'. Master Airscrew vs APC Propeller, which props is better. [Online]. Available at: https://www.rcecho.com/blog/master-airscrew-vs-apc-propeller/ (Accessed: 28/04/2020).

**Merchant, M. P.** (2005) Propeller performance measurement for low Reynolds number unmanned aerial vehicle applications.

**Purushothama Raj, P. & Ramasamy, V.** (2012) 'Strength of materials (Kindle Edition)'.[in Pearson, Upper Saddle River. Available at: https://www.oreilly.com/library/view/strength-of-materials/9789332514829/xhtml/ch6sec6.xhtml (Accessed: 11/02/2020).

**Sherry, L. & Neyshabouri, S.** (2014) 'Estimating takeoff thrust from surveillance track data', Transportation Research Board Annual Meeting.

**Simons, M.** (1999) Model Aircraft Aerodynamics. 4th Edition edn. Swanley : Nexus Special Interests.

**Toman, U. T., Hassan, A.-K. S., Owis, F. M. & Mohamed, A. S.** (2019) 'Blade shape optimization of an aircraft propeller using space mapping surrogates'. Advances in Mechanical Engineering, 11 (7), pp. 1687814019865071.

**Traub, L.** (2016) 'Simplified propeller analysis and design including effects of stall'. The Aeronautical Journal, 120 (1227), pp. 796-818.

**Ugural, A. C.** (2009) Stresses in beams, plates, and shells. CRC press.

**Weakley, L.** (2018) 'Selecting propellers'. [Online]. Available at: http://www.theparkpilot.org/selecting-propellers (Accessed: 06/11/2019).

**Weick, F. E.** (1930) Aircraft propeller design. McGraw-Hill Book Company, inc.